Challenge Journal of CONCRETE RESEARCH LETTERS

Vol.13 No.4 (2022)

acoustic emission aerated concrete compressive strength concrete corrosion cracking curing ductility durability energy absorption ferrocement fly ash fracture mechanical properties mortar nanoparticle palm oil fuel ash reinforced concrete self-compacting concrete silica fume strengthening superplasticizer tensile strength workability waste disposal water absorption

ISSN 2548-0928

TULPAR ACADEMIC PUBLISHING

Challenge Journal of Concrete Research Letters

E-mail: *cjcrl@challengejournal.com*

Web page: *cjcrl.challengejournal.com*

TULPAR Academic Publishing
www.tulparpublishing.com

Challenge Journal of Concrete Research Letters

CONTENTS

Research Articles

TULPAR ACADEMIC PUBLISHING

Challenge Journal of Concrete Research Letters

Research Article

Effect of steam–curing on the glass fiber reinforced concrete

Mehmet Canbaz [a,*], Mouad Bensaoud [b], Hakan Erol [a], Hasan Selim Şengel [a]

[a] *Department of Civil Engineering, Eskişehir Osmangazi University, 26480 Eskişehir, Türkiye*

[b] *Department of Civil Engineering, University of Tripoli, R6XF+46G Tripoli, Libya*

ABSTRACT

Due to the increased need to use precast concrete to reduce construction duration and to accelerate the cement reaction process to achieve the required concrete resistance that enables the elements to gain the required strength to handle the loads generated by the transportation process, many companies use steam curing methods to expedite the hydration process. The steam curing process negatively affects the concrete strength, especially in the long term. Fibers of different types are used to improve the interior composition of concrete and increase its crack resistance. The purpose of the current study was to determine the effect of the glass fiber on the behavior of steam-cured concrete. In this study, 90 concrete cubes were used with 15cm dimensions, three different weight ratios of glass fibers (0%, 0.12%, and 0.24%) with two curing methods standard curing in the water tank (water curing - WC) for 3, 7, and 28 days, and steam curing (SC) for 4 and 8 hours. Nine specimens of each mix were cast in 12 mm and 24 mm fibers length and tested for each curing duration and method. The results of this study indicate that fiber glass addition to the steam-cured concrete has a positive effect on the concrete unit weight and the ultrasonic pulse velocity. Moreover, the result showed that the tensile and compressive strength of the concrete has been positively affected by the length of the fiber more than the fiber weight percentage.

ARTICLE INFO

Article history:
Received 22 July 2022
Revised 20 August 2022
Accepted 2 September 2022

Keywords:
Precast concrete
Steam curing
Glass fiber
GFRC

1. Introduction

Nowadays the need for precast concrete buildings has increased as some countries are facing severe housing shortages and labor shortages as well (Liu et al. 2020). Due to rising construction costs and the increasing importance of quality and timely delivery, many developers are choosing innovative construction techniques such as precast concrete structures, which can speed up the construction process in less time (Zeyad et al. 2021; Canbaz et al. 2022). Precast concrete needs a long time, up to days, to reach the resistance that enables it to withstand the stresses resulting from the transportation process from the precast concrete supplier to the construction site, which causes an increase in the duration of project implementation and reduces the production capacity of the precast concrete (Liu et al. 2019). However, Steam curing is mainly used to produce prefabricated components in many concrete structures. The steam curing method is characterized by improving the mechanical properties of concrete at an early age (Yang et al. 2021). On the other hand, this process has negative effects as the accelerated hydration reaction of concrete results in poor durability and long-term load-bearing capacity (Yoo et al. 2016). Recently, researchers focused on ways to improve the mechanical properties and durability of steam-cured concrete by various methods such as mechanical treatment by reducing the rate of temperature change and also improving mechanical properties by adding concrete additives or fibers to the concrete mix (Yu et al. 2016; Vairagade et al. 2012).

Fiber additives play a major role in mechanical properties improvement, such as toughness and crack growth resistance abilities (Brandt 2008; Won et al. 2012). Fibers improve concrete in all directions since fibers are scattered randomly in the concrete during mixing

* *Corresponding author*. Tel.: +90-222-239-3750 ; Fax: +90-222-239-3613 ; E-mail address: mcanbaz@ogu.edu.tr (M. Canbaz)
ISSN: 2548-0928 / DOI: https://doi.org/10.20528/cjcrl.2022.04.001

(Tassew and Lubell 2014; Balaguru and Shah 1992). Previous research has established that improving the post-peak ductility by adding fibers also improves eliminating temperature and shrinkage cracks, pre-crack tensile strength, impact strength, and fatigue strength (Vandewalle 2000; Vairagade and Kene 2012). Traditionally, many types of fibers have been used in fiber reinforcement concrete FRC, each of these types has a different impact on the concrete mechanical behavior based on fiber shape, size, strength, and type, common types are carbon, steel, glass, and natural fibers. Several applications of FRC use fibers that make up about 1% of the concrete volume (Tan et al. 2012; Banthia 2003).

The use of fiber glass in concrete reinforcement was first introduced by researchers in Russia in the 1940s then used in the construction industry in 1970 in the United Kingdom. Chandramouli et al. (2010) and Shah and Rangan (1994) observed increases in compressive strength of 20–25 percent and flexural and splitting tensile strength of 15–20 percent in their studies on glass fiber reinforcement concrete. Similar results were found by Tassew and Lubell (2014) who found that regardless of the mix composition or fiber length, the volume proportion of glass fiber (GF) increased the flexural strength of ceramic concrete. Regardless of the fiber length or mix composition, ceramic concrete's compression toughness index, flexural toughness, and shear toughness all significantly increased with an increase in fiber content (Tassew and Lubell 2014; Shende and Pande 2011).

Several attempts have been made to research the effect of glass fiber on the mechanical properties of the GFRC. Previous research on the effect of steam curing (Kohno et al. 2009) examined the mechanical properties of GFRC samples that were steam-cured for 1-5 hours and then kept in standard curing for 90 days. In our study, however, micro glass fibers were incorporated into the GFRC sample mix, and the effect of longer steam curing (such as 8-hour curing) was investigated. Microfibers are important in controlling microcracks that may occur especially in long-term steam curing applications. This paper attempts to focus on the effect of glass fiber on the steam cured concrete. In this study cube specimen of 15 cm dimensions was used to examine the effect of different fiber lengths and weight percentage on the unit weights, the ultrasonic pulse velocity, the compressive strength, and the split tensile strength of the concrete.

2. Experimental Study

2.1. Materials

Concrete cube specimens were created by using three types of crushed aggregates. Fig. 1, shows an analysis of the particle size of the aggregate mixture. The commercial quartz sand as fine aggregate (specific gravity of 2.65). Further, the densities of the fine aggregates were 2.69, 2.70, and 2.71 g/cm^3, for fine aggregate sizes of (0-4 mm), (4-11.2 mm), and (11.2-22.4 mm) respectively.

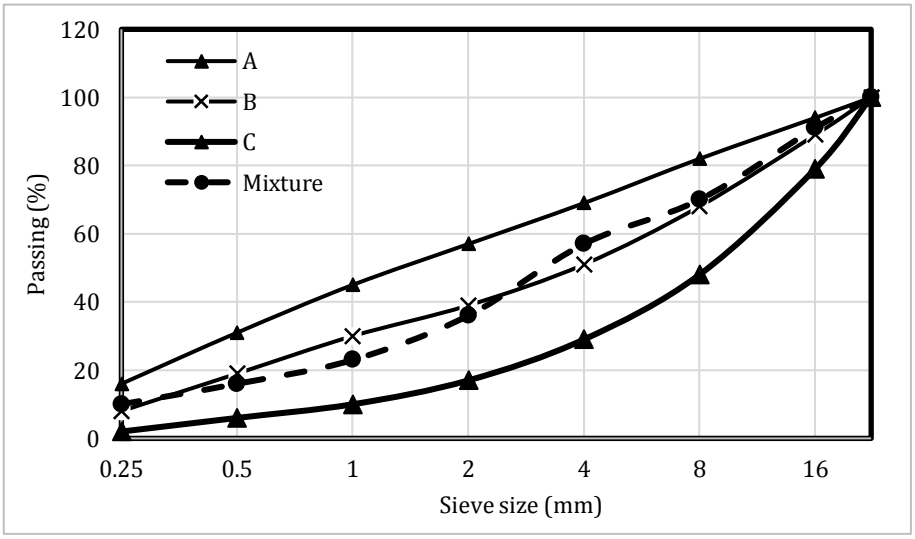

Fig. 1. Granulometry of the aggregate mixture according to EN 12620.

To improve the workability of concrete and avoid the loss in strength during the excess use of water, superplasticizers were used as an admixture and the properties of the new generation of superplasticizers are shown in Table 1. Furthermore, the physical and chemical properties of tap water used in mixing the specimens are given in Table 2.

Table 1. Properties of admixture.

Chemical structure	Appearance	Cl, %	pH	Density, g/cm^3	Alkali, %
Polycarboxylic ether	Brown	≤ 0.10	5-7	1.069-1.109	≤ 3.00

Table 2. Properties of mixing water.

Chemical property, mg/l						Physical property	
Al	0,04	Cu	0,016	Ni	5,07	Conductivity, µS/cm	628
NO_3	11,1	Fe	0,007	K	6,8	Hardness, Fd^0	30,11
NH_4	0,06	Mn	0,015	As	1,19	pH	7,35

The mechanical properties of the glass fiber reinforcements (Fig. 2) used in the concrete mix were as follows, 3400 MPa tensile strength, 77 GPa modulus of elasticity, and a density of 2.60 kg/dm^3, however, the diameter of the glass fiber was 13-15 µm with two different lengths 12, and 24 mm.

Portland cement type CEM I 42.5 R was provided by a local supplier with physical and chemical properties shown in Table 3.

2.2. Method and tests

Cube specimens of 15 cm were created to examine the effect of glass fiber with different lengths and weights, three different weight ratios of glass fibers (0%, 0.12%, and 0.24%) were used in two different lengths 12, and 24 mm. Table 4 shows the mix ratio of 1m^3 concrete mixture by weight. Two curing methods were implemented in the study, standard curing in the water tank (water curing - WC) for 3, 7, and 28 days, and steam curing (SC) for 4, and 8 hours. The group of WC was demolded 24 h after casting and then put in a water tank at 20 C and was taken out of the tank 3 hours before the test. Nine specimens of each mix were cast in 12 mm, and 24 mm fibers length and tested for each curing duration and method, eventually reaching 90 specimens.

To examine the changes in the unit weight, ultrasonic pulse velocity, splitting tensile strength, and compressive strength, tests were carried out for each fiber ratio, length, curing condition, and duration, as can be seen in Figs. 3 and 4. However, the test results will be discussed in further sections.

Fig. 2. Glass fiber.

Table 3. Properties of cement.

Chemical properties				Physical properties	
SiO_2	19.2	K_2O	0.63	Density, g/cm^3	3.09
Al_2O_3	4.56	Na_2O	0.31	Specific surface, cm^2/g	3190
Fe_2O_3	3.09	SO_3	3.21	Setting time (initial), min	163
CaO	62.9	CI-	0.01	Setting time (final), min	228
MgO	1.88	LOI	3.8	Soundness, mm	1

Table 4. A mix ratio of 1 m^3 of concrete mixture by weight.

Cement (kg)	Water (kg)	Superplasticizer (kg)	Aggregate (kg)		
			0-4 mm	4-11.2 mm	11.2-22.4 mm
435	125	3.5	967	333	555

3. Discussion

The effect of glass fiber length and fiber ratio on the unit weight of concrete is shown in Fig. 5. When the fiber ratio increases, the unit weight of the concrete increases as well. Depending on the fiber rate of increase, the increase in unit weight increased by 1.8% in the samples with 12 mm fiber, while the increase rate reached 1.4% when the fiber size reached 24 mm. On the other hand the increase of the curing time, causes the decrease in the unit weight with the addition of fiber. Depending on the time of curing, the unit weight increased up to 2.08% regardless of fiber ratio and fiber length. Concrete unit weight is expected to decrease due to water loss in con-

crete exposed to drying in construction site conditions. However, during the experiment, the samples are kept in water to simulate standard curing conditions, as a consequence of the samples being removed from the curing tank 2-3 hours before the test and the surface is allowed to dry, which caused an increase in the unit weight due to the water it contains.

Fig. 3. Mechanical tests.

Fig. 4. Ultrasonic pulse velocity and mechanical tests.

Fig. 6 shows the change in UPV (ultrasonic pulse velocity) depending on fiber ratio, fiber length, and curing time. The UPV is increased by 11%, with the increase in the fiber content. The bridging of gaps and cracks induced by the fibers causes the UPV to increase as the waves caused by UPV have passed through the gaps in a short time. Since it takes time for the gaps to fill and the internal structure to gain strength during hydration, fibers with 24mm length were more effective in passing through these gaps at an early age. This effect disappeared on the 28th day, and similar results were obtained with an increase in the UPV which was dependent on the fiber ratio and independent of the fiber length.

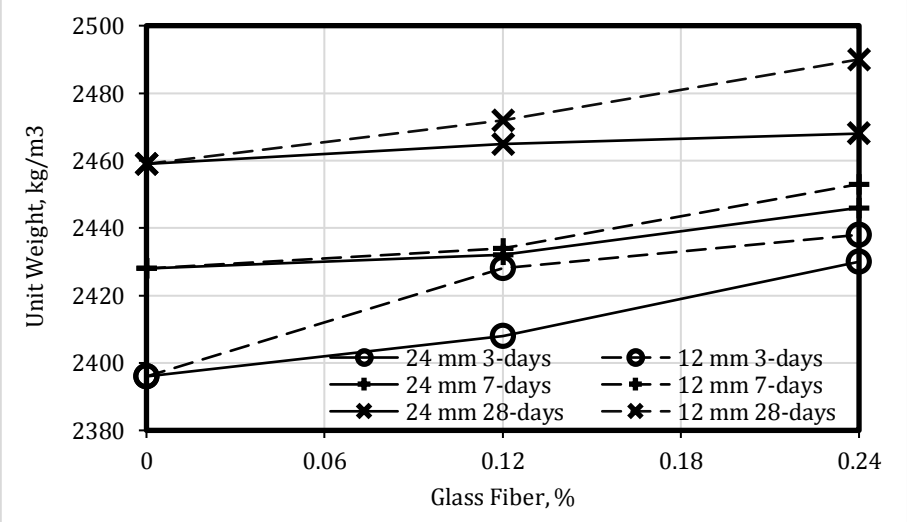

Fig. 5. Unit weight of glass fiber concrete.

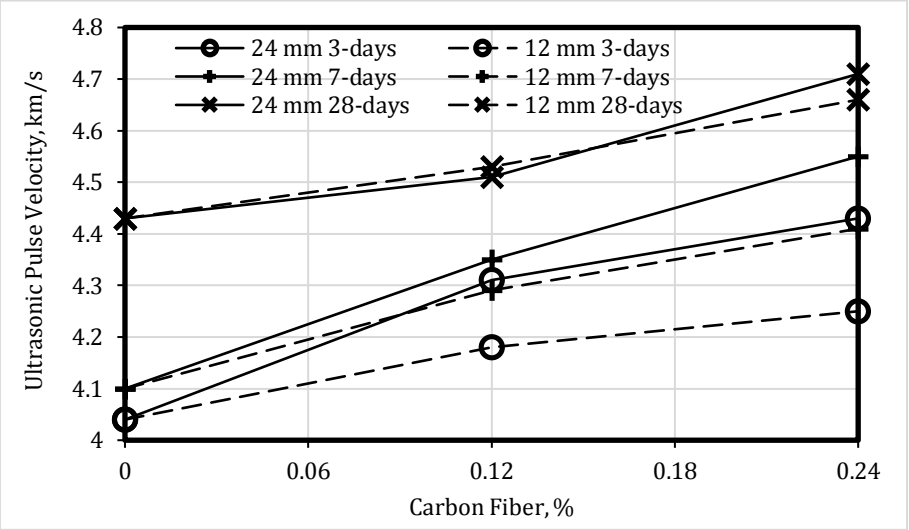

Fig. 6. UPV test results of glass fiber concrete.

The compressive strength of the glass fiber concrete samples is given in Fig. 7. It can be seen that when the short fiber was used with the concrete, the compressive strength of the 3-day curing increased by 13%. However, the increase rate decreased by 11% and 5.6% in the 7-day and the 28-day curing respectively. In the case of using long fiber, the compressive strength of concrete increased by 37%, 42%, and 17% in the 3-day, 7-day, and 28-day respectively. The fibers caused an increase in compressive strength by controlling the growth of microcracks in the concrete under pressure stress with the effect of bridging. Since these fibers have a smooth surface, they cannot show sufficient adherence. For this reason, the compressive strength of the concrete increases depending on the length of the fiber. Due to the concrete not gaining enough strength at an early age, glass fibers can withstand more stress, where the contribution to strength is more in these fibers. Additionally, compared to the 28-day reference samples, the compressive strength of the 3-day and 7-day were 63% and 72% respectively. On the other hand, when the fiber was added the compressive strength of the samples reached 74% on the 3-day and 89% on the 7-day. Therefore, using glass fiber in concrete caused a significant increase in strength, especially at an early age.

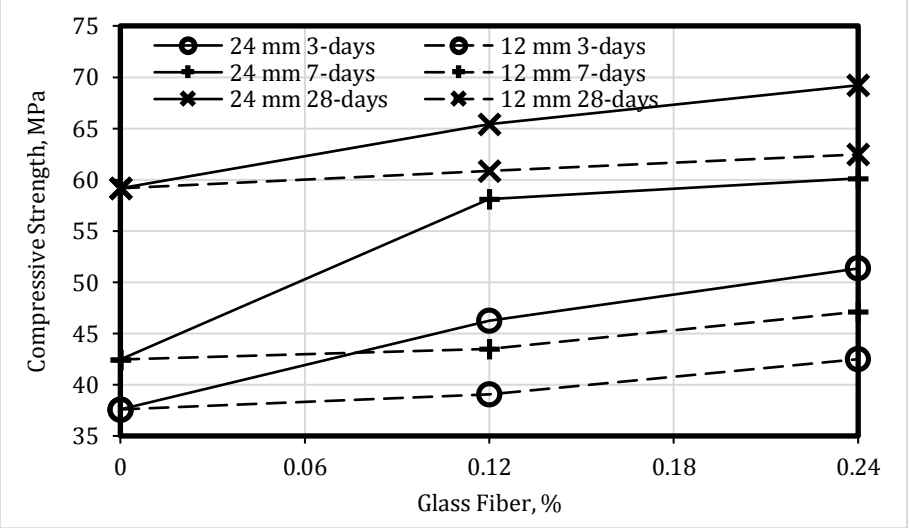

Fig. 7. Compressive strength of glass fiber concrete.

Fig. 8 illustrates the result of splitting tensile strength of glass fiber reinforced concrete under the indirect method of assessing the tensile strength (Brazilian test), the result shows that the splitting tensile strength increased by 24% when the short fibers were added to the concrete. Moreover, this increase reached 40% in the case of long fibers. Generally, when the Brazilian test is carried out to determine the splitting tensile strength, the concrete cracks, and splits under the effect of linear load, although the glass fibers limit this crack by the effect of bridging. However, this positive effect of the fibers is being gradually lost because the fiber was partially ruptured with the increase in the load and due to the loss of adherence. Since adherence is increased with the increase of the length of the fibers, the tensile strength of the samples reinforced by the long fibers witnessed bet-

ter results. Compared to the 28-day reference sample of the splitting tensile strength, the reference samples gained 65% and 81%, while the samples with fiber gained 81% and 93% in 3-days and 8-days respectively. It is observed that it is possible to counteract tensile stresses that occur in the internal structure due to mechanical impacts or effects such as shrinkage at early ages by using glass fibers.

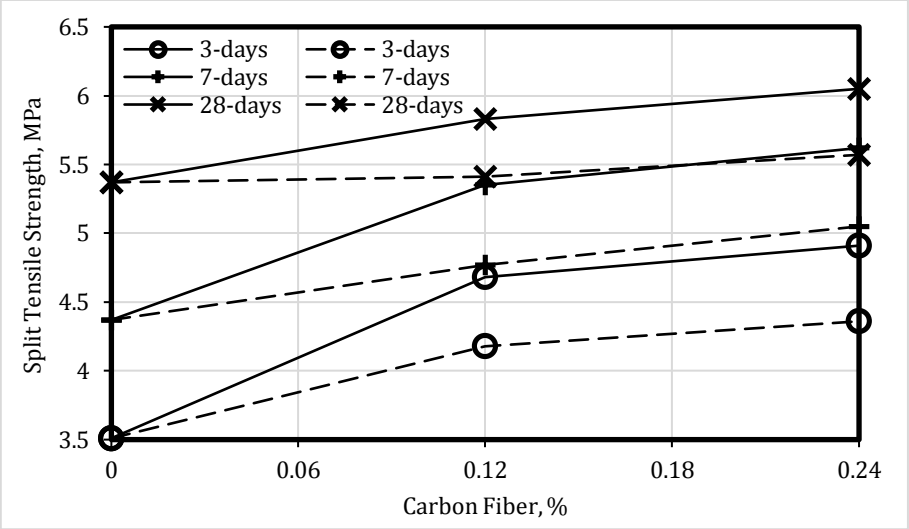

Fig. 8. Splitting tensile strength of glass fiber concrete.

The behavior of fiber-reinforced concrete in the unit weight under the effect of steam curing is given in Fig. 9. The figure shows that the unit weight has increased due to the increase of the fiber under steam curing. However, the unit weight reached 2.4% and 0.7% when using short and long fiber respectively. By contrast, when the samples are compared according to the unit weights of the reference sample, it has been found that the concrete sample without fibers under the steam curing has been decreased by 1.87%, as opposed to the samples with fibers which were reduced by 0.8% and 1.5% for short fibers and long fibers respectively. Overall, the fact that the formation of the internal structure could not be completed in a short time under the effect of steam curing and that it did not provide sufficient filling caused a slight decrease in the unit weights of the reference concrete.

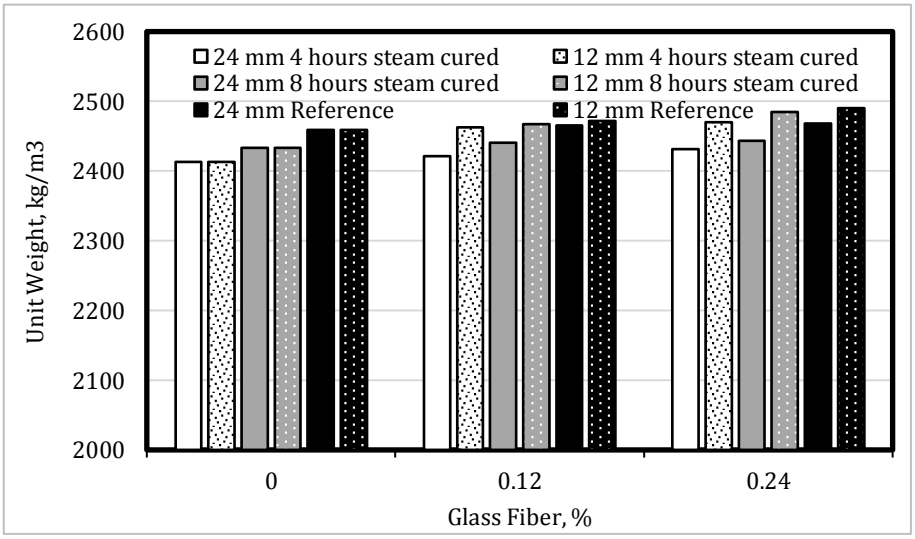

Fig. 9. Unit weight of steam-cured glass fiber concrete under various curing durations.

The variation of UPV values with fiber content and fiber size of reference concretes under steam curing is demonstrated in Fig. 10. It can be seen that when the 12 mm fiber length was used, the samples without steam curing increased by 5.2% compared to the reference sample without fibers, however the percentage of increase was decreased by 2.5% in case of steam curing. On the other hand, when the 24 mm fiber length has used the samples without steam curing increased by 6.3%, and as opposed to the short fibers, the long fibers caused an increase by 8.1% in UPV compared to the reference samples. UPV can take low values due to cracks or gaps

in the concrete. However, fiber addition increases the UPV values as it makes it easier to overcome these gaps. Since steam curing is aimed to accelerate the hydration reaction to gain early strength in the concrete, which ultimately increases the UPV, further, these values can be increased with the addition of fibers. However, the irregularity in the fiber distribution causes the UPV increase to occur in different ways in the samples.

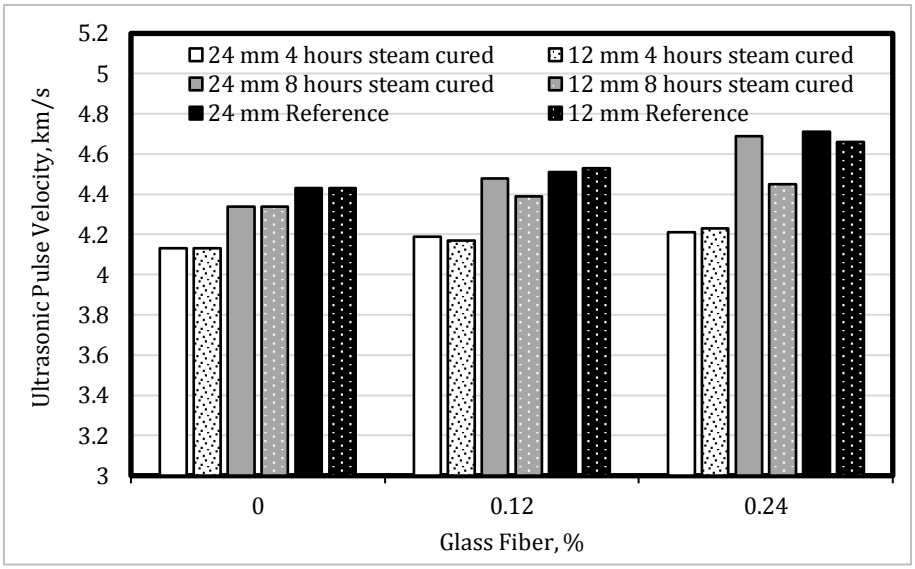

Fig. 10. UPV test results of steam-cured glass fiber concrete under various curing durations.

The variation of steam cured fiber reinforced concrete with compressive strength of 28-day reference fiber concrete is demonstrated in Fig. 11. In the case of using short fibers, the compressive strength of the reference samples under standard curing has increased by 57%, although in the case of steam curing this increase reached 63%. On the other hand, when the long fiber was used, the compressive strength of the reference samples increased by 17%, while this increase was 30% in the steam-cured samples. Furthermore, the glass fibers were used to control the micro cracks that may occur in the internal structure during the early strength gain phase in the steam curing application, and it has caused a great increase in the compressive strength as well. Additionally, in standard curing, it was observed that the glass fiber size and distribution have an effect on the concrete compressive strength, and since the amount of glass fibers is higher when using short fibers with the same ratio as long fibers, the increase in the amount of fibers causes better distributing of the fibers in the internal structure of the concrete which enhances the compressive strength. It can be seen that with the application of 8 hours of steam curing, the samples without fibers gain reached 64% in compressive strength, while the samples with short and long glass fibers gained 98% and 71% respectively.

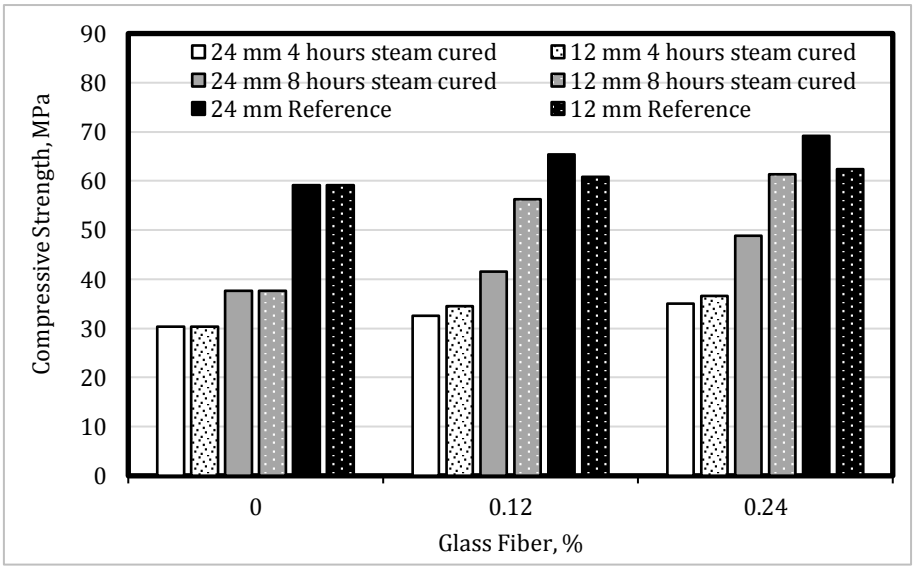

Fig. 11. Compressive strength of steam-cured glass fiber concrete under various curing durations.

Split tensile values with variations of fiber ratio and size of reference concrete under steam curing are given in Fig. 12. It can be seen that with the addition of short glass fiber in the reference concrete without steam curing, the splitting tensile strength increased up to 3.7%, however, with the application of steam curing the increase rate reached 45.9%. And in the case of long glass fiber, the splitting tensile strength of the reference samples increased by 12.7%, while this rate increased to 35.8% in the steam-cured samples. Fiber has been especially effective in steam curing applications, as it prevents the increase of microcracks and voids that occur during the hydration of cement in a short time steam curing application. On the other hand, when the steam curing time was increased, a comparison between the steam curing samples and the 28-day reference samples was conducted, and it has been found that the splitting tensile strength reached 65.4%, 95.3%, and 64.3% without fiber, with short fibers and long fibers respectively. Although it has been found that long fibers did not increase the tensile strength gain with steam curing effect as much as short fibers, the number of fibers is more effective than the fiber length, especially since there are micro-cracks, and short fibers are effective in preventing these cracks.

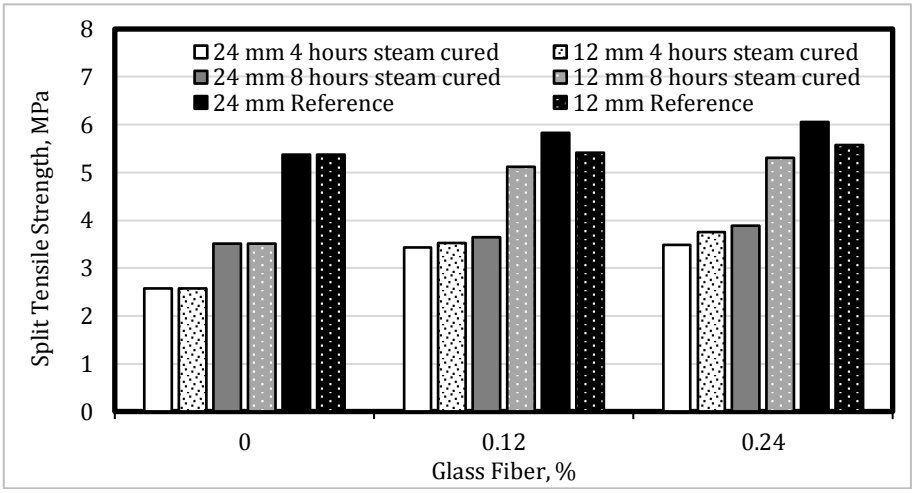

Fig. 12. Splitting tensile strength of steam-cured glass fiber concrete under various curing durations.

4. Conclusions

The conclusions of the study are summarized as follows:

- At the end of the experimental study, considering the glass fiber ratios, when 0.24 % of the fiber is used, the highest values are found in unit weight is around 2490 kg/m^3, 4.71 km/h in UPV, additionally compressive and splitting tensile strength were found to be around 69.2 MPa and 6.05 MPa respectively. However, when comparing the mechanical and physical properties between the 0.12 % and 0.24 %, it has been found that using 0.24% fiber was advantageous. Therefore, it is recommended to use 0.24% fiber.
- When the study is conducted in terms of fiber length, it has been found that the highest values of samples reinforced with short glass fiber are 2468 kg/m^3 in unit weight, 4.71 km/h in UPV, 69.2 MPa in compressive strength, and 6.05 MPa in split tensile strength, on the other hand, the highest values of samples reinforced with long glass fiber are 2490 kg/m^3 in unit weight, 4.66 km/h in UPV, 62.5 MPa in compressive strength, and 5.57 MPa in splitting tensile strength. Therefore, long fibers are recommended due to their advantages in mechanical properties.
- For prefabricated building applications where steam curing is inevitable, and when curing time and fiber ratio are taken into account, the increase in fiber ratio is advantageous, and it has been observed that an 8-hour curing application is advantageous if 0.24 % fiber is used. The results of 8-hour steam curing reached 2485 kg/m^3 in unit weights, 4.69 km in UPV /h, 61.3 MPa compressive strength, and 5.31 MPa in splitting tensile strength. The experiments have shown that using fibers with steam curing had a positive effect on the mechanical properties, especially in compressive strength which is the most effective parameter in the application of prefabricated buildings.
- Considering the steam curing and fiber length, it was observed that the mechanical properties of the samples increased significantly in the 8-hours steam curing compared to the 4-hours steam curing. In the case of 8-hour steam curing, the compressive strengths of short fiber samples reached 61.3 MPa, while it reached 48.9 MPa in long fiber samples. On the other hand, the splitting tensile strength reached 5.31 MPa in short fiber samples, while it reached 3.89 MPa in long fiber samples. It can be said that it is more advantageous to use short fiber for a fixed ratio in steam curing applications.

As a result of the study, it has been revealed that fiber use is important in steam curing applications and fiber size was as effective as fiber ratio. For steam curing application, using 0.24% short glass fiber in samples is recommended. However, for further studies, it is recommended to repeat the experiments by increasing the fiber ratio and shortening the fiber size, especially for cost optimization. In addition, it is recommended to carry out studies not only in terms of short-term properties but also in terms of long-term properties.

Acknowledgements

None declared.

Funding

The authors received no financial support for the research, authorship, and/or publication of this manuscript.

Conflict of Interest

The authors declared no potential conflicts of interest with respect to the research, authorship, and/or publication of this manuscript.

References

Balaguru PN, Shah SP (1992). Fiber Reinforced Cement Composites. McGraw-Hill Inc.

Banthia N (2003). Crack growth resistance of hybrid fiber composites. *Cement and Concrete Composites,* 25, 3–9.

Brandt AM (2008). Fibre reinforced cement-based (FRC) composites after over 40 years of development in building and civil engineering. *Composite Structures,* 86, 3–9.

BS EN 12620 (2002). Aggregates for concrete. British Standards Institution, London, United Kingdom.

Canbaz M, Bensaoud M, Erol E, Sengel HS (2022). Effect of carbon fibers on the mechanical properties of steam-cured concrete. *Challenge Journal of Structural Mechanics,* 8(2), 38–46.

Chandramouli K, Srinivasa RP, Pannirselvam N, Seshadri ST, Sravana P (2010). Strength properties of glass fiber concrete. *Engineering Applications,* 5(4), 1–6.

Kohno K, Amo K, Kawahito K (2009), Influence of steam curing condition on glass fiber reinforced concrete using GFRC cement. *J-STAGE,* 38(431), 939–945.

Liu B, Jiang J, Shen S, Zhou F, Shi J, He Z (2020). Effects of curing methods of concrete after steam curing on mechanical strength and permeability. *Construction and Building Materials,* 256, 119441.

Liu M, Tan H, He X (2019). Effects of nano-SiO_2 on early strength and microstructure of steam-cured high volume fly ash cement system. *Construction and Building Materials*, 194, 350–359.

Shah SP, Rangan VK (1994). Effect of fiber addition on concrete strength. *Indian Concrete Journal,* 5, 13–21.

Shende A, Pande A (2011). Comparative study on steel fiber reinforced cum control concrete. *International Journal of Advanced Engineering Sciences and Technologies,* 6, 116–120.

Tan C, Hamid R, Kasmuri M (2012). Dynamic stress-strain behaviour of steel fiber reinforced high-performance concrete with fly ash. *Advances in Civil Engineering,* 907431, 1–6.

Tassew ST, Lubell AS (2014). Mechanical properties of glass fiber reinforced ceramic concrete. *Construction and Building Materials,* 51, 215–224.

Vairagade V, Kene K (2012). Experimental investigation on hybrid fiber reinforced concrete. *International Journal of Engineering Research and Applications,* 2, 1037–1041.

Vairagade V, Kene K, Deshpande N (2012). Investigation of compressive and tensile behavior of fibrillated polypropylene fibers reinforced concrete. *International Journal of Engineering Research and Applications*, 2, 1111–1115.

Vandewalle L (2000). Cracking behaviour of concrete beams reinforced with combination of ordinary reinforcement and steel fibers. *Materials and Structures,* 33, 164–170.

Won JP, Hong BT, Choi TJ, Lee SJ, Kang JW (2012). Flexural behaviour of amorphous micro-steel fibre-reinforced cement composites. *Composite Structures,* 94, 1443–1449.

Yang J, Hu H, He X, Su Y, Wang Y, Tan H, Pan H (2021). Effect of steam curing on compressive strength and microstructure of high volume ultrafine fly ash cement mortar. *Construction and Building Materials,* 266, 120894.

Yoo DY, Banthia N, Yoon YS (2016). Flexural behavior of ultra-high-performance fiber-reinforced concrete beams reinforced with GFRP and steel rebars. *Engineering Structures,* 111, 246–262.

Yu R, Spiesz P, Brouwers HJH (2016). Energy absorption capacity of a sustainable ultra-high performance fibre reinforced concrete (UHPFRC) in quasi-static mode and under high velocity projectile impact. *Cement and Concrete Composites,* 68, 109–122.

Zeyad AM, Johari MAM, Alharbi YR, Abadel AA, Abadel YHM, Tayeh BA, Abutaleb A (2021). Influence of steam curing regimes on the properties of ultrafine POFA-based high-strength green concrete. *Journal of Building Engineering,* 38, 102204.

Challenge Journal of Concrete Research Letters

Research Article

Economical evaluation of reinforced concrete hospital construction cost using bottom ash and fly ash

Burak Oz [a,*], Memduh Karalar [a], Murat Çavuşli [a]

[a] *Department of Civil Engineering, Zonguldak Bülent Ecevit University, 67100 Zonguldak, Türkiye*

ABSTRACT

The use of waste materials in nature (e.g. fly ash, bottom ash) in the construction phase of buildings is of great importance both in terms of environmental pollution and the construction cost of the structures. Therefore, in this study, the effects of bottom ash and fly ash on the construction cost of reinforced concrete (RC) hospital buildings are investigated by considering experimental tests and 3D nonlinear analyzes. During the experiments, four different concrete series are created and fly ash and bottom ash are added to replace 0–5 mm grain size aggregates in the concrete mixture at different ratios. The RC beams created according to four different concrete series are subjected to experimental tests. Afterward, it is determined that the most critical mixing ratio for RC beams subjected to experimental tests is selected as 75% bottom ash ratio and fly ash. For the purpose Ankara Bilkent City Hospital is selected for 3D nonlinear seismic analyses and the hospital structure is subjected to 10 various earthquake analyses. This study showed that there was a noticeable decrease in the construction cost when the costs of the hospital structure were compared as a result of the earthquake analysis. Another important point is that the use of bottom ash and fly ash is thought to contribute to savings in the energy to be used for the storage of wastes by causing less electrical energy use in cement production, less greenhouse gas emissions, natural raw material consumption and nature pollution.

ARTICLE INFO

Article history:
Received 9 August 2022
Revised 14 September 2022
Accepted 29 September 2022

Keywords:
Construction cost
Construction management
Finite element analysis
Fly ash
Bottom ash

1. Introduction

In many countries of the world, thermal power plants are built to produce energy, and millions of waste ash are generated from these thermal power plants every year. In these thermal power plants, coal is used for electricity generation and the coal ash generated as a result of production must be recycled in order not to harm the environment. However, the bottom ash and fly ash that is created in thermal power plants are thrown into nature and cause pollution of people's health and the environment. For this reason, recycling these waste materials is of great importance for the health of future generations. When coal burns in a thermal power plant, it leaves ash behind. Some falls to the bottom of the furnace, which is called bottom ash and some is carried upwards by the hot combustion gases of the furnace and held by the filter, which is called fly ash. The use of fly ash as recycled material can provide economic and environmental benefits (Epri 1998); using fly ash in building materials and concrete technology might solve the problems of industrial waste, environmental pollution, and destruction of thousands of acres of land and also offers the opportunity to create cost-effective new building materials (Zekić et al. 2014). Fly ash reduces CO2 emissions and is considered an environmentally friendly material because it can be used as a byproduct in Portland cement and various building materials and can be a cost-effective replacement for Portland cement in many markets (Rodriguez 2021). Tiles and bricks are made from fly ash emit 90% less carbon dioxide (Transparency Market Research 2019). When fly ash mixed with lime and water, it forms a compound similar to Portland cement and this makes fly ash suitable for the base material in blended cement,

* *Corresponding author*. Tel.: +90-372-291-2619 ; Fax: +90-372-257-4023 ; E-mail address: burak.oz@beun.edu.tr (B. Oz)
ISSN: 2548-0928 / DOI: https://doi.org/10.20528/cjcrl.2022.04.002

mosaic tiles, and hollow blocks (Rodriguez 2021). Fly ash can be partially used in concrete mixtures as a cement substitute and no need to grind and no need drying like trass. By using fly ash, less electrical energy will be used for cement production and so energy savings will be achieved. Since fly ash is a very thin material, it increases the workability of concrete as well (Arioğlu and Manzak 1992). Since the use of fly ash in cement ensures less use of cement clinker, it has environmental benefits such as less greenhouse gas emissions, less consumption of natural raw materials, less pollution of nature, energy saving used in the storage of waste, as well as technical benefits such as high-strength concrete and low hydration temperature (Cement Research and Application Center).

One of the most common uses of fly ash is plain Portland cement concrete (PCC) coating. Road construction projects using PCC can use large amounts of concrete, and the additive of fly ash provides significant economic benefits. More than 50% of concrete placed in the USA contains fly ash (Rodriguez 2021). The Ministry of Environment and Urbanization of Türkiye states that in accordance with the general technical specification for construction, there should be a minimum of 250 kg/m^3 cement and 50 kg/m^3 fly ash to be used in the roller compacted concrete mixture. Additionally, according to the general technical specifications for reinforced concrete works, it is recommended that mineral additives such as fly ash should not exceed 30% of the cement amount in order not to deteriorate the permeability property of concrete (Directorate of High Technics Board 2018).

Bricks composed of fly ash can be produced in various strengths and sizes, and be found in building walls etc. Besides their traditional uses, bricks composed of fly ash can also be used for the construction of various infrastructure projects such as roads and sidewalks, dams and bridges (Attarde et al. 2014). In addition, it can be used in concrete additives, fine aggregate, coarse aggregate, light aggregate, clay additive, brick binder material, aerated concrete blocks, concrete panels, concrete, glass, wood and ceramics (Güler et al. 2005; Aruntaş 2006; Transparency Market Research 2019).

According to the data obtained from the Provincial Environmental Status Reports prepared by the Provincial Directorates of Environment and Urbanization, the total amount of coal used in thermal power plants in 2015 was around 60,666,000 tons, and the fly ash and bottom ash produced was approximately 17,710,000 tons (Republic of Türkiye Ministry of Environment and Urbanisation 2016). According to another statistic, the results of Thermal Power Plant Water, Wastewater and Waste Statistics Survey in 2018, 26.1 Million tons of waste was generated in 55 active thermal power plants with an installed power of 100 megawatts (MW) and above, 87.5% of which was sent to ash mountain or ash dam, and 12.4% was sent to licensed waste processing facilities and used for backfilling of mines, while 0.1% was disposed of by other methods (TURKSTAT 2019).

There are very few studies in the literature about the recycling of fly ash and bottom ash and their effects on construction costs such as Chindaprasirt et al. (2009), Rafieizonooz et al. (2016), Canpolat et al. (2004), Andrade et al. (2007, 2009), Siddique et al. (2012), Abdulmatin et al. (2018), Boonserm et al. (2012), Kim and Lee (2011), Garcia-Lodeiro et al. (2016), Wongsa et al. (2016), Jurič et al. (2006), Albitar et al. (2015), Aruntaş (2006), Ashish et al. (2018), Baspinar et al. (2014), Cavusoglu et al. (2021), Dinelli et al. (1996), Verma et al. (2016, 2019), Wang et al. (2016), Wu et al. (2014), and Yost et al. (2013). In these studies, the effects of fly ash material on the structural behavior of the structures have been investigated and it has been concluded that fly ash material has great effects on both the structural and cost of the structures.

As seen from these studies, very few investigators have examined the effects of various fly ash and coal bottom ash ratios on the construction cost of structures in the past. Besides, there are very few studies about the effects of various fly ash and coal bottom ash ratios on the 3D seismic behavior of hospital structural elements (beams, columns) in the literature. For this reason, this study is of great importance to overcome these gaps in the literature.

2. Scope of the Study

In this study, the effects of different fly ash and bottom ash ratios on the construction cost of structures are investigated in detail. For this aim, firstly, four various concrete beams with different fly ash and bottom ash ratios are created in the laboratory (Karalar 2020). After pure concrete is generated, fly ash and bottom ash are used instead of aggregate in pure concrete. The fly ash ratios used in pure concrete are 25%, 50%. Moreover, the bottom ash ratio utilized in pure concrete is 75%. Then, these beams are subjected to a bending test. The most critical beam (concrete with 75% coal bottom ash) is taken as a reference and the properties of this reference concrete material are used for structural elements of a hospital to examine the effects of coal bottom ash ratios on the construction cost of RC hospital structures. For this aim, the existing hospital building is modeled with the mechanical properties of the 75% bottom ash substitution and the carrier system has been reanalyzed, except for the foundation system. Then, earthquake analysis is performed and it is observed that the hospital structure is not damaged in the earthquake as dimensions of the columns and beams in the hospital structure used coal bottom ash added to the concrete are reduced. And then, the cost has been compared between concrete with 75% bottom ash substitution and without bottom ash in the current design. From this result, it is concluded that as concrete with 75% coal bottom ash is used in hospital structures, there will be a significant reduction in the cost of hospital structures and this recycling will make a significant contribution to the country's economy.

3. Preparation of the Reinforced Concrete Beams

In Zonguldak-Türkiye, coal is produced since the 1900s and this produced coal is sent to both other provinces and countries. For this reason, a coal-fired thermal power plant (Çates) was established in Zonguldak to

turn coal into energy. The waste coal bottom ash produced in this coal-fired thermal power plant is released to nature every day and causes great damage to nature. Therefore, recycling of this coal bottom ash is of great importance both for Türkiye's economy and the health of people living located in the Zonguldak. In this study, the contribution of the addition of coal bottom ash, which is waste in nature, to the construction cost of hospital structures is investigated both experimentally and numerically. Experimentally, the concrete material is prepared in the laboratory and 75% coal bottom ash ratio is added instead of aggregate in the prepared concrete materials. Besides, 25% and 50% coal fly ash ratios are added instead of aggregate in the concrete materials. As a result of this experiment, 75% bottom ash ratio is determined as the most critical ash ratio. Details of the concrete samples prepared in the laboratory are presented in Table 1. As can be seen from Table 1, sample 1 represents pure concrete and other samples represent additive concretes. Coal bottom ash has been used in the concrete mix to replace aggregates of 0-5 mm grain size. Details of the materials used in 4 different concrete beams are presented in Table 2. Components in the cement and weight per unit of components are presented in Table 3.

Table 1. Concrete samples for various bottom ash ratios (Karalar 2020).

Sample number	Statement
1	Pure concrete
2	%25 fly ash
3	%50 fly ash
4	%75 bottom ash

Table 2. Components in the concrete samples and weight per unit of components (Karalar 2020).

Components	Weight per unit of volume (%)
Portland Cement Clinker	45 – 64
Limestone	0 – 5
Gypsum	3 – 6
Calcium Oxide	0 – 5
Magnesium Oxide	0 – 5
Natural Pozzolan	36 – 55

Table 3. Components in the cement and weight per unit of components (Karalar 2020).

Material	Reference (kg)	75% Bottom ash (kg)	25% Fly ash (kg)	50% Fly ash (kg)
Cement	9.0	9.0	6,75	4,500
Water	4.77	4.77	4.77	4.77
Fly ash	0.0	0.0	1,294	2,588
Bottom ash	0.0	11,312	11,312	11,312
0-5 mm aggregate	23.1450	5.7854	5.7854	5.7854
5-15 mm aggregate	12.7320	12.7320	12.7320	12.7320
15-25 mm aggregate	21.9900	21.9900	21.9900	21.9900
Chemical admixture	0.1200	0.1200	0.1200	0.1200
Unit weight of concrete	71.7570	65.7107	64,755	63,799

For the reinforced concrete samples, bottom ash is obtained from Zonguldak coal-fired thermal power plant and added to the concrete materials. The capacity of this coal-fired thermal power plant is 2x150 MW. Approximately 1.500.000 tons of coal is burned annually in this factory. At the end of this burning process, tons of ash are formed annually. 4 different concrete sample mixes are mixed in the concrete mixer and the concrete consistency is adjusted. Concrete samples were placed in cube molds in the laboratory and kept in water for 28 days (Fig. 1).

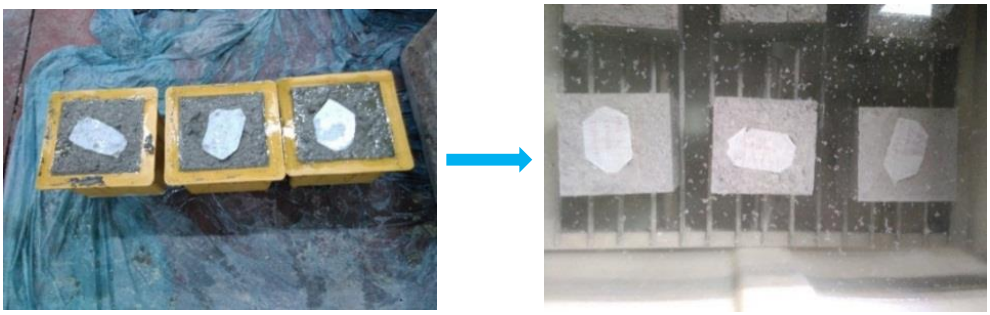

Fig. 1. Preparation of concrete samples in the laboratory (Karalar 2020).

Fig. 2 shows that how concrete beams and beam molds are prepared in the laboratory. 4 different reinforced concrete beam molds are prepared in a private laboratory. The dimensions of the 4 different beam molds are equal and the beam mold dimensions are 300 x 400 x 2000 mm. Total of 10 different stirrups are used in concrete beams and the distances between stirrups are 200 mm. Besides, the diameter of stirrups is 8 mm. 2 compression reinforcements are placed on the concrete beams to ensure stirrup connections. These compression reinforcement bars have a diameter of 12 mm. In addition, 3 tension reinforcements are placed at the bottom of the beam molds and the diameter of these tension bars is 12 mm. After a total of 4 different beams are prepared in the laboratory, a total of 28 days are waited for the concrete to reach the desired hardness, and after 28 days, the beam molds are removed (Karalar 2020).

Fig. 2. Preparation of molds for concrete beams (Karalar 2020).

4. Experimental Test Set-up and Results

Used devices for crack and flexure analyses of concrete beams are shown in Fig.3. Four different RCBs prepared in the special laboratory are subjected to flexure and crack tests. Flexure and crack test results for all beams are presented in Fig. 3. According to Fig. 3, the maximum crack width for pure concrete is 3.17 cm. Besides, the maximum distance between the vertical cracks was 15 cm in the reference concrete beam. In Fig. 3, the flexure and crack test results of the beam prepared by adding 75% coal bottom ash into concrete instead of aggregate are presented. According to Fig. 3, the maximum crack width is 2.82 cm and the maximum crack length is 39 cm. From this result, it is seen that when coal bottom ash is added to the concrete, the crack width and crack length decrease. Furthermore, the maximum crack width on the beam is 3.16 cm and the maximum crack length is 32 cm. In Fig. 3, test results of the beam prepared by adding 50% coal fly ash to the aggregate in the concrete are presented. If 50% of coal fly ash is added instead of aggregate in the concrete inside the beam, the maximum crack width is 3.38 cm and the maximum crack length is 24 cm. It is clear from these results that the most critical threshold value for four different ash ratios used instead of aggregate in concrete is 75% coal bottom ash ratio. From this result, it is concluded that using 75% coal bottom ash ratio in reinforced concrete structures may cause less damage in the RC structures (Karalar 2020).

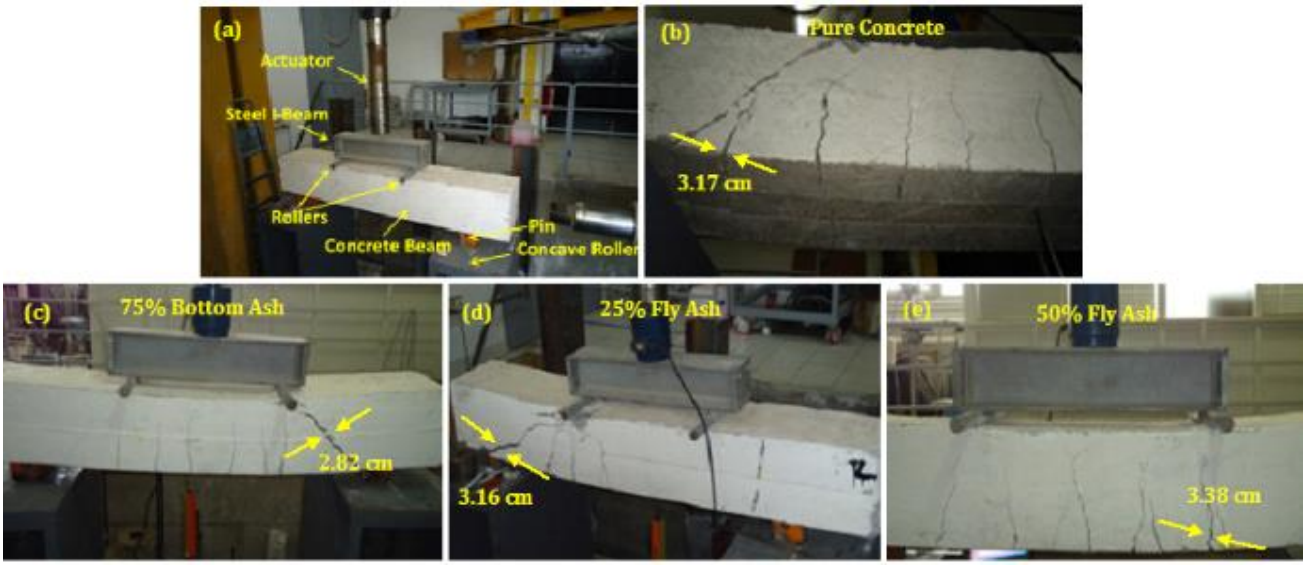

Fig. 3. Crack and flexure behavior of reference concrete beam: (a) Static testing apparatus; (b)Pure concrete; (c) 75% Bottom ash; (d) 25% Fly ash; (e) 50% Fly ash (Karalar 2020).

5. 3D Earthquake Analysis Results

This section, it is aimed to investigate the effects of the 75% bottom ash ratio in the concrete on the 3D seismic behavior of hospital buildings. For this aim, a 10 story hospital structure is selected for 3D modeling and this building is modeled as 3D using SAP2000 software based on the finite element method (Carhoglu 2022). The hospital building was built in Ankara. The general view of Ankara Bilkent city hospital used in 3D analyzes is presented in Fig. 4. 3D model of the building is shown in Fig. 5.

Fig. 4. General view of Ankara Bilkent city hospital (URL-1 2022).

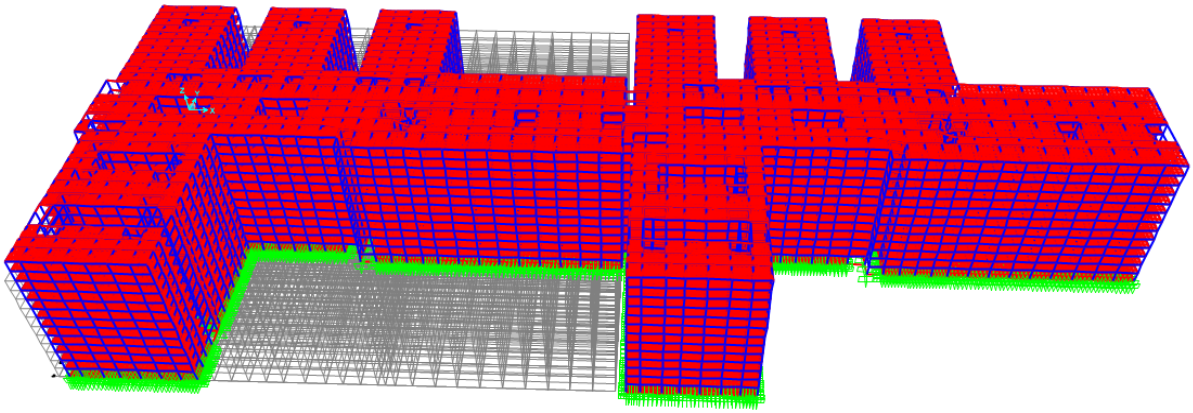

Fig. 5. View of 3D model of the hospital building.

Table 4. Mechanical properties of various earthquakes.

Earthquake record station	d (km)	PGA	PGV	Ap/Vp	TPV	TP
1999 Chi-Chi Earthquake 1	17.8	0.17	59	2.83	6.5	6.0
1999 Chi-Chi Earthquake 2	18.1	0.25	46	5.33	1.4	1.3
1979 Imperial Valley Earthquake 1	0.5	0.30	91	3.23	3.0	3.1
1979 Imperial Valley Earthquake 2	0.6	0.46	109	4.14	3.2	3.8
1979 Imperial Valley Earthquake 3	1.0	0.38	91	4.10	3.4	3.9
1995 Kobe Earthquake	0.6	0.60	74	7.95	0.8	1.4
1989 Loma Prieta Earthquake	5.1	0.48	45	10.46	0.8	0.7
1986 North Palm Spring Earthquake	8.2	0.59	73	7.93	1.1	1.4
1994 Northridge Earthquake 1	7.1	0.45	93	4.75	2.0	3.2
1994 Northridge Earthquake 2	7.1	0.33	67	4.83	1.8	1.9

3D earthquake analysis results are shown in Table 5. As Table 5 is examined, the earthquake analysis results for the current situation of the structure and the earthquake analysis results for the coal bottom ash added situation of the RC structure are presented separately. 3D earthquake analyses are performed under 10 different earthquakes. According to 10 different earthquake analysis results, no damage is obtained in the structural elements for the current situation of the building. From this result, it is concluded that the existing bearing columns and beams are sized appropriately for these earthquakes. Besides, provided that the dimensions of the existing bearing elements of the structure remain constant, it has been observed that if 75% of the coal bottom ash is added to the aggregate in the bearing elements of the structure, no damage will occur for 10 different earthquakes. When the size of the columns and beams is reduced by 10% ratio for the structure with coal bottom ash, there is no damage to the building for 10 different earthquakes. No damage is observed in the structure for 10 different earthquakes in the case of reducing the dimensions of the carrier elements by 20%, 30%, 40% ratios for the structure with coal bottom ash. However, if the dimensions of the bearing elements for the coal bottom ash added structure is reduced by 50% ratio, the structure is damaged for the 1999 Chi-Chi earthquake, 1989 Loma Prieta earthquake, 1986 North Palm earthquake, 1994 Northridge earthquake. In this case, it is concluded that the reduction ratio that should be taken as reference is 40% ratio. From this result, it is concluded that if 75% ratio of coal bottom ash is used instead of aggregate in the structures, the carrying elements of the structure can be reduced by 40% ratio, and if the carrier elements are reduced by 40% ratio, the structure may resist earthquakes. It is understood from this result that if 75% ratio of coal bottom ash waste material is used in concrete material of RC structures, it will cause a significant decrease in the cost of the building (Table 5).

Table 5. Earthquake analysis results for current situation and coal bottom ash added situation.

Earthquake	Current situation of structure	Reduction ratio for structural elements (beams and columns)					
		10%	20%	30%	40%	50%	60%
1999 Chi-Chi Earthquake 1	+	+	+	+	+	+	-
1999 Chi-Chi Earthquake 2	+	+	+	+	+	-	-
1979 Imperial Valley Earthquake 1	+	+	+	+	+	-	-
1979 Imperial Valley Earthquake 2	+	+	+	+	+	-	-
1979 Imperial Valley Earthquake 3	+	+	+	+	+	+	-
1995 Kobe Earthquake	+	+	+	+	+	+	-
1989 Loma Prieta Earthquake	+	+	+	+	+	+	-
1986 North Palm Spring Earthquake	+	+	+	+	+	-	-
1994 Northridge Earthquake 1	+	+	+	+	+	+	-
1994 Northridge Earthquake 2	+	+	+	+	+	-	-

6. Effects of the Construction Cost

For cost comparisons shown in this section of the study, the analyses, unit prices and transport formulas published by the Ministry of Environment, Urbanization and Climate Change of Türkiye are used. Sand, crushed stone and cement are brought from the closest mine and factory to the construction site at a distance of 16 km and 160 km shown in Table 6 and 7. The bottom ash and fly ash is brought from the Catalagzi Thermal Power Plant at a distance of 70 km shown in Table 8, which is also assumed that it will be taken free of charge except the transportation fee. Tables 9 and 10 show the approximate unit costs of one cubic meter of reference concrete and one cubic meter of concrete prepared using bottom ash and fly ash, respectively. The cost comparison between bottom ash and fly ash used in cement mortar and reference concrete for the current design can be seen in Table 11 and the cost comparison between the current design and the more economic design can be seen in Table 12. The density of sand or crushed stone is taken into account in calculations as 1.6 tons/m^3 to convert ton to m^3.

Unit prices of plant-mixed concrete in Tables 9 and 10 are calculated using the construction unit prices and analyses of the Ministry of Environment and Urbanization of Türkiye. The calculated unit prices show approximate market prices and may vary.

It has been seen in the laboratory experiments that when bottom ash and fly ash with 150 kg cement is used in cement mortal, much more compressive strength, and much more flexural and tensile strength than the reference concrete with 300 kg cement in one cubic meter are obtained. Also, of the unit weight is approximately 10 % less than the reference concrete.

Firstly, in this case it is considered no change in the sizes of load-bearing structural elements in the current design shown in Table 11, it is compared the structure costs when using reference concrete or bottom ash and fly ash in cement mortal. It is seen that the structure cost when bottom ash and fly ash used in the concrete is approximately 10% less.

Table 6. Transportation of 1 m^3 of sand or crushed stone to the construction site.

Name of analysis: Sand or crushed stone transportation (m^3)					
Item/group #	Entries	Metric	Quantity	Unit price	Sum ($)
19.100.2495	F = A x K x (0.0007 x M+0.01) x G				1.97
A	Difficulty coefficient		1.00		
G	Density of sand and crushed stone	ton/m^3	1.60		
10.110.1003	K: Motor vehicle carriage coefficient	$	58.10		
M	Transportation distance	km	16.00		
15.100.1002*	Loading, unloading and storing of 1 m^3 of material.	m^3	0.80	0.517	0.41
*If the material on the construction site is available, 80% of the transportation cost will be paid.					
				Transportation and labor cost	2.38
Note: Density of cement is not taken into account in the calculation because no conversion is needed.					

Table 7. Transportation of 1 ton of cement to the construction site.

Name of analysis: Cement transportation (ton)					
Item/group #	Entries	Metric	Quantity	Unit price	Sum ($)
19.100.2495	F = A x K x (0.0007 x M+0.01)				7.09
A	Difficulty coefficient		1.00		
10.110.1003	K: Motor vehicle carriage coefficient	$	58.10		
M	Transportation distance	km	160.00		
15.100.1001*	Loading, unloading and stowing of 1 ton of cement	ton	0.50	2.797	1.40
* Loading fee is deducted for ex-factory materials * If the loading is done at the factory, half of the unit price will be deducted.					
				Transportation and labor cost	8.49
Note: Bottom ash and fly ash is brought from Catalagzi Thermal Power Plant and density of them is not taken into account in the calculation because no conversion is needed.					

Table 8. Transportation of 1 ton of bottom ash or fly ash to the construction site.

Name of analysis: Bottom ash or fly ash transportation (ton)					
Item/group #	Entries	Metric	Quantity	Unit price	Sum ($)
19.100.2495	F = A x K x (0.0007 x M+0.01)				3.43
A	Difficulty coefficient		1.00		
10.110.1003	K: Motor vehicle carriage coefficient	$	58.10		
M	Transportation distance	km	70.00		
15.100.1002*	Loading, unloading and storing of 1 m^3 of material.	m^3	0.80	0.517	0.41
*If the material on the construction site is available, 80% of the transportation cost will be paid.					
				Transportation and labor cost	3.84

Table 9. Unit price of 1 m³ of plant-mixed reference concrete including transportation.

Item #	Definition	Metric	Quantity	Unit price	Sum ($)
Material (cement mortar):					
10.130.1026	Sand	m³	0.482	4.15	2.00
Sand transportation		m³	0.482	2.38	1.15
10.130.1029	Crushed stone (up to 32 mm)	m³	0.723	6.17	4.46
Crushed stone transportation		m³	0.723	2.38	1.72
10.130.1204	Portland cement (bulk)	ton	0.300	35.78	10.73
Portland cement transportation		ton	0.300	8.49	2.55
10.130.9991	Water	m³	0.159	1.23	0.20
10.300.2004	Plasticizing-air entraining mortar fluid admixture on the job	kg	4.000	0.70	2.80
Labor:					
Pumping and pouring:					
19.100.1059	Hourly rate of an automatic concrete plant (1000 L capacity, 50 m³/hour)	h	0.0200	7.51	0.15
10.100.1015	Concrete master	h	0.3000	3.06	0.92
10.100.1063	Expert laborer	h	0.3000	2.39	0.72
10.100.1051	Driver	h	0.6000	3.12	1.87
10.100.1055	Machine operator	h	0.6000	3.59	2.16
10.100.1057	Assistant operator	h	0.6000	2.95	1.77
10.160.1026	Diesel fuel	kg	1.4250	0.89	1.27
10.160.1030	Electric power	kWh	8.7500	0.12	1.01
10.100.1062	Unskilled construction worker	h	5.0000	2.24	11.19
Compacting and protecting:					
19.100.1033	Hourly rate of a concrete vibrator	h	0.3125	4.23	1.32
10.130.9991	Water for curing	m³	0.5000	1.23	0.62
10.100.1015	Concrete master	h	0.9375	3.06	2.87
Sampling and Laboratory Tests:					
10.100.1060	Foreman	h	0.3125	4.49	1.40
10.100.1062	Unskilled construction worker	h	0.3125	2.24	0.70
				Material and labor cost	53.58
				10% contractor's profit and 15% overheads	13.39
				Price per m³	66.97

In the another case it is considered the mechanical properties of the bottom ash and fly ash mix and it is designed the structure more economically. It is seen in Table 12 that the cost difference increases significantly (approximately %25 less).

7. Conclusions

In this study, it has been investigated whether bottom ash and fly ash thrown into nature as waste material from a thermal power plant can be used in reinforced concrete structures and if so, what its effect is on construction costs. In the current design (built structure), the cost of concrete used in the Load-bearing structural is calculated as $3,614,078, and the cost of concrete with bottom ash and fly ash mix in concrete is $3,230,033, so the difference is $384,045 which will be approximately 10% less than the built structure. If the building had been designed considering the mechanical properties of the bottom ash and fly ash, then the cost difference would have been $923,939 (3,614,078-2,690,134), which is approximately 25% less. This is because the increase in strength allows the sizes of load carrying elements to be designed more economically. The fly ash market is estimated to generate 11,371 Million US Dollars in revenue in the United States by 2026 (Transparency Market Research 2019). Türkiye produced 95 Million cubic meters of ready-mixed concrete in 2020 according to Turkish Ready-Mixed Concrete Association (2020) and according to Türkiye Statistical Institute in the year of 2018 data, 22,861,242 cubic meters of coal waste (fly ash, bottom

ash and boiler slag) from power plants was disposed (TURKSTAT 2019). If bottom ash and fly ash had been used in approximately ten Million cubic meters of concrete, 4.634 Million tons of bottom and fly ash (10 Million * 0.4634 ton/m3) would have been used and the cost difference in concrete would have been $56.9 Million US Dollars (10 Million * $5.69). An-other important point is that, by using bottom ash and fly ash, less electrical energy will be used for cement production and energy consumption will be reduced considerably. In addition, it has environmental benefits such as less greenhouse gas emissions, less consumption of natural raw materials, less pollution of nature, energy saving used in the storage of waste and reduction the disposal costs.

Table 10. Unit price of 1 m^3 of plant-mixed concrete with bottom ash and fly ash including transportation.

Item #	Definition	Metric	Quantity	Unit price	Sum ($)
	Material (cement mortar):				
10.130.1026	Sand	m^3	0.121	4.15	0.52
	Sand transportation	m^3	0.121	2.38	0.30
10.130.1029	Crushed stone (up to 32 mm)	m^3	0.723	6.17	4.46
	Crushed stone transportation	m^3	0.723	2.38	1.72
10.130.1204	Portland cement (bulk)	ton	0.150	35.78	6.71
	Portland cement transportation	ton	0.150	8.49	1.59
N/A	Fly ash	ton	0.0863	0.00	0.00
	Fly ash transportation	ton	0.0863	3.84	0.72
N/A	Bottom ash	ton	0.3771	0.00	0.00
	Bottom ash transportation	ton	0.3771	4.80	0.90
10.130.9991	Water	m^3	0.1590	1.23	0.20
10.300.2004	Plasticizing-air entraining mortar fluid admixture on the job	kg	4.000	0.70	2.80
	Labor:				
	Pumping and pouring:				
19.100.1059	Hourly rate of an automatic concrete plant (1000 L capacity, 50 m^3/hour)	h	0.0200	7.51	0.15
10.100.1015	Concrete master	h	0.3000	3.06	0.92
10.100.1063	Expert laborer	h	0.3000	2.39	0.72
10.100.1051	Driver	h	0.6000	3.12	1.87
10.100.1055	Machine operator	h	0.6000	3.59	2.16
10.100.1057	Assistant operator	h	0.6000	2.95	1.77
10.160.1026	Diesel fuel	kg	1.4250	0.89	1.27
10.160.1030	Electric power	kWh	8.7500	0.12	1.01
10.100.1062	Unskilled construction worker	h	5.0000	2.24	11.19
	Compacting and protecting:				
19.100.1033	Hourly rate of a concrete vibrator	h	0.3125	4.23	1.32
10.130.9991	Water for curing	m^3	0.5000	1.23	0.62
10.100.1015	Concrete master	h	0.9375	3.06	2.87
	Sampling and Laboratory Tests:				
10.100.1060	Foreman	h	0.3125	4.49	1.40
10.100.1062	Unskilled construction worker	h	0.3125	2.24	0.70
				Material and labor cost	47.89
				10% contractor's profit and 15% overheads	11.97
				Price per m^3	59.86

Table 11. Cost comparison between bottom ash and fly ash used in cement mortar and reference concrete for the current design.

Load-bearing structural elements	Concrete volume	Reference concrete	Concrete with bottom ash & fly ash
	m^3	($/$m^3$)	($/$m^3$)
Column	5,859.899	$66.97	$59.86
Beam	8,671.321		
Slab	14,855.303		
Foundation	24,576.039		
Total	53,962.562	$3,614,078	$3,230,033
Difference		$384,045	

Table 12. Cost comparison between the current design and the more economic design.

Load-bearing structural elements	Current design		New design	
	Concrete volume	Reference concrete	Concrete volume	Concrete with bottom ash & fly ash
	m^3	($/$m^3$)	m^3	($/$m^3$)
Column	5,859.899	$66.97	4,394.776	$59.86
Beam	8,671.321		7,983.826	
Slab	14,855.303		13,488.680	
Foundation	24,576.039		19,075.541	
Total	53,962.562	$3,614,078	44,942.824	$2,690,134
Difference			$923,939	

Acknowledgements

None declared.

Funding

The authors received no financial support for the research, authorship, and/or publication of this manuscript.

Conflict of Interest

The authors declared no potential conflicts of interest with respect to the research, authorship, and/or publication of this manuscript.

References

Abdulmatin A, Tangchirapat W, Jaturapitakkul C (2018). An investigation of bottom ash as a pozzolanic material. *Construction and Building Materials*, 186, 155-162.

Albitar M, Visintin P, Mohamed Ali MS, Drechsler M (2015). Assessing behaviour of fresh and hardened geopolymer concrete mixed with Class-F fly ash. *KSCE Journal of Civil Engineering*, 19(5), 1445-1455.

Andrade LB, Rocha JC, Cheriaf M (2007). Evaluation of concrete incorporating bottom ash as a natural aggregates replacement. *Waste Management*, 27(9), 1190-1199.

Andrade LB, Rocha JC, Cheriaf M (2009). Influence of coal bottom ash as fine aggregate on fresh properties of concrete. *Construction and Building Materials*, 23(2), 609-614.

Arioğlu E, Manzak O (1992). Economic analysis of fly ash use in the construction sector. *Türkiye Prefabricated Union*, 22, 25-33.

Aruntaş HY (2006). The potential of fly ash usage in construction sector. *Journal of the Faculty of Engineering and Architecture of Gazi University*, 21(1), 193-203.

Ashish DK, Verma SK, Singh J, Sharma N (2018). Strength and durability characteristics of bricks made using coal bottom and coal fly ash. *Advances in Concrete Construction*, 6(4), 407-422.

Boonserm K, Sata V, Pimraksa K, Chindaprasirt P (2012). Improved geopolymerization of bottom ash by incorporating fly ash and using waste gypsum as additive. *Cement and Concrete Composites*, 34(7), 819-824.

Baspinar MS, Demir I, Kahraman E, Gorhan G (2014). Utilization potential of fly ash together with silica fume in autoclaved aerated concrete production. *KSCE Journal of Civil Engineering*, 18(1), 47-52.

Carhoglu AI (2022). Investigation of the interaction of the tank structures exposed to earthquake with the soil. *Hittite Journal of Science and Engineering*, 9 (1) 45–56

Canpolat F, Yılmaz K, Köse MM, Sümer M, Yurdusev MA (2004). Use of zeolite, coal bottom ash and fly ash as replacement materials in cement production. *Cement and Concrete Research*, 34(5), 731-735.

Cavusoglu I, Yilmaz E, Yilmaz AO (2021). Additivity effect on properties of cemented coal fly ash backfill containing water-reducing admixtures. *Construction and Building Materials*, 267, 121021.

Cement Research and Application Center. (n.d.). Mineral Additive-Fly Ash. Mersin: Cimsa. Retrieved from https://www.cimsa.com.tr/ca/docs/4FE58AA58E3A4B7B85FA9E4EE011A8/0F1225956F804377AC3B5D8C47EDC0A8.pdf.

Chindaprasirt P, Jaturapitakkul C, Chalee W, Rattanasak U (2009). Comparative study on the characteristics of fly ash and bottom ash geopolymers. *Waste Management*, 29(2), 539-543.

Dinelli G, Belz G, Majorana CE, Schrefler BA (1996). Experimental investigation on the use of fly ash for lightweight precast structural elements. *Materials and Structures*, 29, 632-638.

Epri (1998). Coal Ash: Its Origin, Disposal, Use, and Potential Health Issues. Palo Alto, CA: EPRI's Environment Division. Retrieved from http://www.coal-ash.co.il/docs/BR-111026.pdf.

Garcia-Lodeiro I, Carcelen-Taboada V, Fernández-Jiménez A, Palomo A (2016). Manufacture of hybrid cements with fly ash and bottom ash from a municipal solid waste incinerator. *Construction and Building Materials*, 105, 218-226.

Güler G, Güler E, İpekoğlu U, Mordoğan H (2005). Fly ash properties and uses. *Türkiye 19th International Mining Congress and Expo*, IMCET, İzmir.

Jurič B, Hanžič L, Ilić R, Samec N (2006). Utilization of municipal solid waste bottom ash and recycled aggregate in concrete. *Waste Management*, 26(12), 1436-1442.

Karalar M (2020). Experimental and numerical investigation on flexural and crack failure of reinforced concrete beams with bottom ash and fly ash. *Iranian Journal of Science and Technology, Transactions of Civil Engineering*, 44 (Suppl 1), 331–354.

Kim HK, Lee HK (2011). Use of power plant bottom ash as fine and coarse aggregates in high-strength concrete. *Construction and Building Materials*, 25(2), 1115-1122.

Rafieizonooz M, Mirza J, Salim MR, Hussin MW, Khankhaje E (2016). Investigation of coal bottom ash and fly ash in concrete as replacement for sand and cement. *Construction and Building Materials*, 116, 15-24.

Republic of Türkiye Ministry of Environment and Urbanisation (2016). State of the Environment Report for Republic of Türkiye. Retrieved from Türkiye Environmental Status Report: https://webdosya.csb.gov.tr/db/ced/editordosya/tcdr_ing_2015.pdf.

Rodriguez J (2021). The Pros and Cons of Using Fly Ash in Your Concrete. Retrieved 02 10, 2021, from Uses, Benefits, and Drawbacks of Fly Ash in Construction: https://www.thebalancesmb.com/fly-ash-applications-844761.

Siddique R, Aggarwal P, Aggarwal Y (2012). Influence of water/powder ratio on strength properties of self-compacting concrete containing coal fly ash and bottom ash. *Construction and Building Materials*, 29, 73-81.

Transparency Market Research. (2019). Fly Ash Market to Generate Revenue of US$11,371 Mn by 2026, Economic Benefits Add Impetus to the Market. Retrieved from https://www.prnewswire.com/news-releases/fly-ash-market-to-generate-revenue-of-us11-371-mn-by-2026--economic-benefits-add-impetus-to-the-market---tmr-300906289.html.

Turkish Ready-Mixed Concrete Association (2020). Türkiye Ready Mixed Concrete Industry Statistics. Retrieved from https://www.thbb.org/sektor/istatistikler/.

TURKSTAT (2019). Thermal Power Plant Water, Wastewater and Waste Statistics. Retrieved 01 06, 2021, from Türkiye Statistical Institute News Bulletin: https://data.tuik.gov.tr/Bulten/Index?p=Termik-Santral-Su,-Atiksu-ve-Atik--Istatistikleri-2018-30674.

URL-1 (2022). https://www.ccnholding.com/en/construction/ankara-city-hospital-bilkent/

Verma S, Amritphale SS, Khan MA (2019). Utilization of brine sludge and fly ash waste as complementary resources, for making non-toxic, geopolymeric (cement-free) materials. *Iranian Journal of Science and Technology, Transactions of Civil Engineering*, 43 (Suppl 1), 603–614.

Verma SK, Ashish DK, Singh J (2016). Performance of bricks and brick masonry prism made using coal fly ash and coal bottom ash. *Advances in Concrete Construction*, 4(4), 231-242.

Wongsa A, Zaetang Y, Sata V, Chindaprasirt P (2016). Properties of lightweight fly ash geopolymer concrete containing bottom ash as aggregates. *Construction and Building Materials*, 111, 637-643.

Wang L, Sun H, Sun Z, Ma E (2016). New technology and application of brick making with coal fly ash. *Journal of Material Cycles and Waste Management*, 18, 763–770.

Wu T, Chi M, Huang R (2014). Characteristics of CFBC fly ash and properties of cement-based composites with CFBC fly ash and coal-fired fly ash. *Construction and Building Materials*, 66, 172-180.

Yost JR, Radlin´ska A, Ernst E, Salera M (2013). Structural behavior of alkali activated fly ash concrete. Part 1: mixture design, material properties and sample fabrication. *Materials and Structures*, 46, 435–447.

Zekić V, Tica N, Milić D, Bačkalić Z (2014). Economic characteristics of concrete production from fly ash as a way of land recultivation. *Economics of Agriculture*, 61(1), 63-71.

Challenge Journal of Concrete Research Letters

Research Article

Effects of fibers geometry and strength on the mechanical behavior and permeability properties of slurry infiltrated fiber concrete

Fatih Özalp [a,*]

[a] *Department of Civil Engineering, İstanbul Medeniyet University, 34700 İstanbul, Türkiye*

ABSTRACT

The use of slurry-infiltrated fiber concrete (SIFCON) has been increasing in recent years. SIFCON is a very good alternative, especially in structural reinforcement processes. In this study, the effects of 2 different steel fibers of normal strength (3D) and high strength (5D) with different geometry and strength properties and polyolefin origin synthetic fiber are examined on the mechanical behavior and capillary water permeability properties of SIFCON. Steel fibers were used in 2 different ratios by volume 4% and 8%, while polyolefin synthetic fiber was used at 4% by volume. The bending strength and splitting tensile strength of SIFCON containing 5D steel fiber are 46.47 MPa and 18.47 MPa, respectively, 4.9 and 2.1 times higher than plain concrete. In addition, the fracture energy of SIFCON containing 5D steel fiber is 20400 N/m, and it is 358 times higher than plain concrete, 1.6 and 3.1 times higher than concrete containing the same amount of 3D fiber and polyolefin synthetic fiber, respectively. The capillary water absorption of SIFCON, which contains 4% synthetic fiber and 8% 3D steel fiber by volume, is 0.121 mm and 0.112 mm, respectively, which is higher than all other mixtures in the study. As a result of the study, higher splitting tensile strength, bending strength and fracture energy values were obtained in concretes containing 5D steel fiber, which have high tensile strength and have better adhesion to concrete due to its geometry. The use of synthetic fibers or high amounts of steel fibers increased the permeability.

ARTICLE INFO

Article history:
Received 7 September 2022
Revised 11 October 2022
Accepted 31 October 2022

Keywords:
SIFCON
Steel fiber
Synthetic fiber
Mechanical behavior
Fracture energy
Permeability

1. Introduction

Slurry Impregnated Fiber Concrete (SIFCON) is a fiber-reinforced cementitious composite in which steel or synthetic fibers can be used separately or as a hybrid, with very high tensile and flexural strengths, and can reach extraordinary toughness values (Farnam et al. 2010; Ali and Riyadh 2018; Khamees et al. 2020; Mohan et al. 2020). Its use in many areas such as precast products, elements exposed to impact and dynamic loads, pavements, applications requiring heat resistance, repair and reinforcement works, places that need protection against explosion and fire, and prestressed reinforced concrete beams has recently become widespread. Depending on this situation, studies to determine the mechanical behavior, fire resistance, behavior against dynamic loads, impact resistance for explosion and ballistic effects, and durability to environmental effects of this special type of concrete are increasing day by day (Lankard 1984; Schneider 1992; Tuyan and Yazıcı 2012; Rattan and Singh 2019; Soylu and Bingol 2019).

Steel fibers are widely used to improve the mechanical properties of concrete. Apart from steel fibers, different fibers such as polyolefin, polypropylene, polyethylene, nylon, glass, carbon and basalt fibers can be used to improve the mechanical properties of concrete (Topcu and Canbaz 2007; Sun et al. 2018; Yildizel 2018; Akcay and Ozsar 2019).

Ipek et al. (2019) in their study to examine the mechanical properties of SIFCON, they filled 1/3, 2/3 and 3/3 of the beam molds with fibers. The highest flexural

* *Corresponding author*. Tel.: +90-216-280-3223 ; Fax: +90-216-280-3404 ; E-mail address: fatih.ozalp@medeniyet.edu.tr (F. Özalp)
ISSN: 2548-0928 / DOI: https://doi.org/10.20528/cjcrl.2022.04.003

strength values were reached in the samples using 60mm and 35mm long steel fibers together and in combination of 60mm steel fiber and 50mm polypropylene fiber. Flexural strength values are 44.02MPa and 41.23MPa, respectively. It has been determined that steel and polypropylene fibers are effective in improving the mechanical properties of SIFCON, however, since polypropylene fiber is lighter and its cost is lower than compared to steel fiber, it can provide significant advantages in terms of unit weight and cost.

In their study, Canbaz and Ünüvar (2016) investigated the properties of SIFCON produced with different fibers and binders. Polypropylene fibers and two different lengths of steel fiber were used to investigate the effect of the fiber. Portland cement, fly ash, pozzolanic cement, and calcium aluminate cement were used as binders. The effects of fiber type and binder on the test results were determined by performing unit weight, ultrasonic pulse velocity, bending strength, compressive strength, and water absorption tests on the produced samples. It has been observed that the binder type affects the SIFCON properties. It has been evaluated that the use of steel fiber is more suitable than polypropylene fiber as it improves mechanical properties. It has been determined that macro-sized steel fibers are more effective in improving mechanical properties.

In his study, Al-Mashhadani (2021) produced SIFCON samples with five different fiber types. It was determined that the steel fiber samples gave better flexural strength results compared to the samples reinforced with other fiber types. In addition, when high temperature is applied to the samples, less strength losses occurred in steel fiber reinforced samples compared to other fibrous samples.

Yazıcı et al. (2010) investigated the effects of mineral additives such as Class C fly ash and ground granulated blast furnace slag on the mechanical properties of SIFCON concrete. In addition, they also examined the effects of steel fiber alignment on SIFCON. The test results showed that the use of mineral additives positively affects the mechanical properties of SIFCON and that the alignment of the steel fibers is an important factor in obtaining superior performance.

Yalçınkaya et al. (2014) in their study on SIFCON, stated that many parameters such as fiber type and geometry, curing conditions, properties of the fiber-matrix interface, and matrix strength affect fiber-matrix bond properties. They stated that this bond can be strengthened with mineral additives such as metakaolin. In their study, they determined that the use of metakaolin improved compressive strength and fiber-matrix bond properties. They also determined that hooked fiber performs better than straight fiber.

In his study, Sengul (2018) used hybrid steel fibers recovered from scrap tires to produce SIFCON. The compressive strength, bending strength, and splitting tensile strength of the samples were determined. In addition, the load-displacement curves of the samples were also obtained. The test results showed that the flexural strength and toughness increased as the fiber content increased and the waste steel fibers could be used successfully in SIFCON.

Numerous studies have been carried out in the literature on the use of 3D, 4D and 5D steel fibers in concrete (Gao et al. 2021; Ding et al. 2022). Abdallah et al. (2016) investigated the fracture behavior of concretes with different water/cement ratios containing 3D, 4D and 5D fibers. The results showed that the pull-out load and total pull-out work of mixtures containing 5D fiber were greatly higher than mixtures containing 3D and 4D fibers. In addition, at lower water/cement ratios, the performance of the fibers is much better. Chen et al. (2022) investigated the flexural strength properties of concretes in different strength classes containing varying amounts of 3D, 4D, and 5D steel fibers. The results showed that increased fiber dosage and the number of hooked ends were effective in improving the flexural tensile behavior of concrete beams in general, especially high-strength concrete beams. Venkateshwaran et al. (2018) obtained stress versus crack-mouth-opening and displacement curves of 69 different specimens with multiple hook tip geometry by 3-point bending test. Based on the test results, empirical models were established to determine residual flexural stresses through multiple regression analysis. The results show that residual flexural strengths were found to be proportional to the square root of the concrete compressive strength and the square of the number of hooks at the fiber ends.

Guler and Akbulut (2022) used single-hooked 3D fiber and multi-hooked 4D and 5D steel fibers to evaluate the performance of the fibers at room conditions and after high-temperature effects. As a result of the study highest residual compressive, bending, and residual toughness capacity after high- temperature effect were obtained in the samples using 5D steel fiber.

Studies comparing the performance of steel fibers with polyolefin fibers are also available in the literature (Tagnit-Hamou et al. 2005; Alberti et al. 2014; Enfedaque et al. 2021). In the studies, the mechanical properties and fracture energies of concretes containing steel fiber were higher than concretes containing polyolefin fiber. However, due to the fact that polyolefin fibers are lighter and have less corrosion risk, it is recommended in some studies to use them in concrete as a hybrid with steel fibers (Alberti et al. 2015).

The main aim of this study is to determine the effect of fibers with different geometry and tensile strength on the mechanical behavior and permeability properties of SIFCON. In this context, compressive strength, splitting tensile strength, bending strength, and capillary water absorption tests were performed on the samples. In addition, load-displacement curves of all samples were obtained to determine the fracture energies.

2. Experimental Study

In the study, various SIFCON concrete mixtures were prepared in the laboratory by using different types of steel fibers and macro synthetic fibers. Compressive strength, splitting tensile strength, and bending strength tests were carried out to determine some mechanical properties of SIFCON concrete on cube and beam samples of the prepared concrete mixtures. In addition, the

fracture energy values of all concrete mixtures were determined. For the permeability properties of concrete samples, capillary water absorption tests were carried out. Thus, the effect of fiber type on the mechanical behavior and permeability properties of SIFCON concrete was evaluated by making performance-based comparisons.

2.1. Materials and mix proportions

2.1.1. Cement and aggregates

CEM I 42.5 R type portland cement was used in the study. The aggregate used is a silica-based aggregate with a maximum size of 1 mm. In high-performance concrete, aggregates with silica and quartz properties are frequently preferred because they are stiffness, clean, and highly durable. In this study, the siliceous aggregate was also preferred for its high strength and stiffness. Some physical and chemical properties of cement and silica aggregate used in the study are given in Table 1. The particle size distribution of siliceous aggregate is presented in Table 2.

Table 1. Properties of cement and siliceous aggregate.

	Cement	Siliceous aggregate (0-1 mm)
SiO_2 (%)	20.1	98.1
CaO (%)	63.5	0.3
SO_3 (%)	2.7	0.2
Al_2O_3 (%)	4.2	0.7
Fe_2O_3 (%)	3.2	0.3
MgO (%)	1.3	0.02
Na_2O (%)	0.9	0.01
K_2O (%)	0.2	0.04
Specific gravity (gr/cm^3)	3.16	2.62
Specific surface area (cm^2/gr)	3892	-
Chloride (Cl^-)	0.003	0.010
Activity index, 7 days (%)	-	-
Loss on ignition (%)	3.4	0.2
Particle ratio (<0,045 mm) %	-	-
Insoluble residue (%)	0.4	-

2.1.2. Steel and synthetic fibers

In the mixtures, 2 different steel fibers with normal and high strength and 1 polyolefin origin synthetic fiber were used. Some properties of these fibers are given in Table 3.

The water/cement ratio was kept constant as 0.27 in all SIFCON mixtures. One of the steel fibers used in the mixtures is of normal strength and has a tensile strength of 1100 MPa and the other is high strength and has a tensile strength of 2250 MPa. The polyolefin fiber has a tensile strength of 590 MPa. All fibers were used in the same proportion (4%) by volume in concrete mixtures, and 314 kg/m^3 for steel fibers and 36.4 kg/m^3 for polyolefin synthetic fiber. Siliceous aggregate was used in all mixtures and the maximum particle size is 1 mm. The superplasticizer additive is a high-range water reducer and was used at a rate of 3% by weight to the total binder in all mixtures. It was used the slurry in a flowing consistency with a diameter of 750 mm in all mixtures. The amounts of materials for the concrete mixes were given in Table 4.

Table 2. Particle size distribution (%) of siliceous aggregate.

Sieve size (μm)	Siliceous aggregate (0-1 mm)
+1600	-
1000-1600	0.5
710-1000	4.2
500-710	12.6
355-500	25.2
250-355	32.5
180-250	20.8
125-180	3.1
90-125	0.7
63-90	0.3
0-63	0.1

Table 3. Properties of steel and polyolefin fibers.

	Normal strength steel fiber	High strength steel fiber	Polyolefin fiber
Length (mm)	60	60	50
Diameter (mm)	0.75	0.75	0.50
Aspect ratio	80	80	100
Density (kg/m^3)	7850	7850	910
Modulus of elasticity (MPa)	210000	210000	11000
Tensile strength (MPa)	1100	2250	590

In the coding of the mixtures, it was named as plain concrete mixture (REF), mixture containing normal strength steel fiber (3DSF-4), mixture for high strength steel fiber (5DSF-4) and mixture containing polyolefin (PE-4). In addition, a mixture (3DSF-8) containing 628 kg/m³ (8% by volume) normal strength steel fiber was also prepared to determine the effects of the increase in fiber content on the SIFCON properties. All specimens were taken from the mold after 24 hours and kept in a water-filled curing tank until the test day.

Table 4. Materials used in concrete mixtures.

	REF	3DSF-4	5DSF-4	PE-4	3DSF-8
Cement (kg/m^3)	1000	1000	1000	1000	1000
Silica fume (kg/m^3)	250	250	250	250	250
Siliceous powder (0-1 mm) (kg/m^3)	820	820	820	820	820
Water (kg/m^3)	270	270	270	270	270
Superplasticizer (kg/m^3)	30	30	30	30	30
Normal strength steel fiber	-	314	-	-	628
High strength steel fiber	-	-	314	-	-
Synthetic fiber	-	-	-	36.4	-
Water/Cement	0.27	0.27	0.27	0.27	0.27
Water/Binder	0.22	0.22	0.22	0.22	0.22
Unit Weight (kg/m^3)	2370	2684	2684	2406	2998

Steel fibers used in the study were produced in accordance with EN 14899-1 standard. The hooked ends in all steel fibers ensure the desired fiber is pulled out. This is the mechanism that actually produces the known concrete ductility and post-crack strength. In the high-strength fiber apart from the normal strength fiber, the hook ends are shaped to form the perfect anchorage with the concrete, where the pull-out mechanism from the concrete is replaced by the elongation of the fiber. The tensile strength of a steel fiber has to increase in parallel with the strength of its anchorage. Otherwise, if the strength of the anchor is increased and the tensile strength of the steel fibers is not sufficient, the steel fibers will fracture. The geometry and strength of normal and high-strength steel fibers used in the study are given in Fig. 1 (Bekaert 2021).

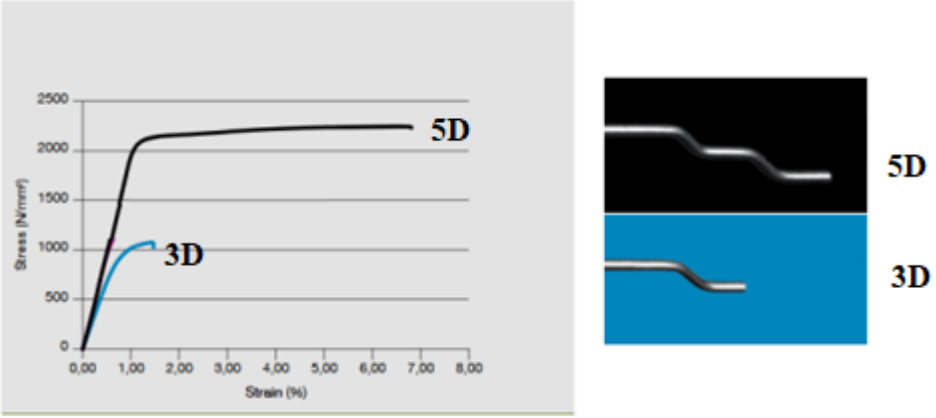

Fig. 1. Geometry and strength of normal and high-strength steel fibers (Bekaert 2021).

2.2. Specimen preparation

In the preparation of the mixtures, first of all, dry cement, silica fume and silica powder aggregate were mixed for 30 seconds. 3/4 of the mixing water was added to the dry materials and mixed for 1 minute. Afterwards, the remaining water and the superplasticizer chemical additive, which has a very high water reducing feature, were mixed in a container and added to the mixture. Thus, a more homogeneous distribution of the chemical

additive was ensured and the dry materials are prevented from absorbing the water of the superplasticizer additive and reducing its effectiveness. The active ingredient ratio of the superplasticizer used in the study was 30%, and 70% water amount was used in calculating the water/cement and water/binder ratios. Therefore, the water/cement ratio in the mixtures was 0.27 and the water/binder ratio was 0.22. Schematic flow diagram of SIFCON is given Fig. 2. Finally, the fibers used in the study were placed in the molds in determined amounts and the prepared slurry was poured into the steel molds (Fig. 3). Within the scope of the study, compressive strength, splitting tensile strength, and capillary water absorption tests were performed on the samples. In addition, the 3-point bending test was applied to the samples, and the bending strength and fracture energy test results of the samples were also determined.

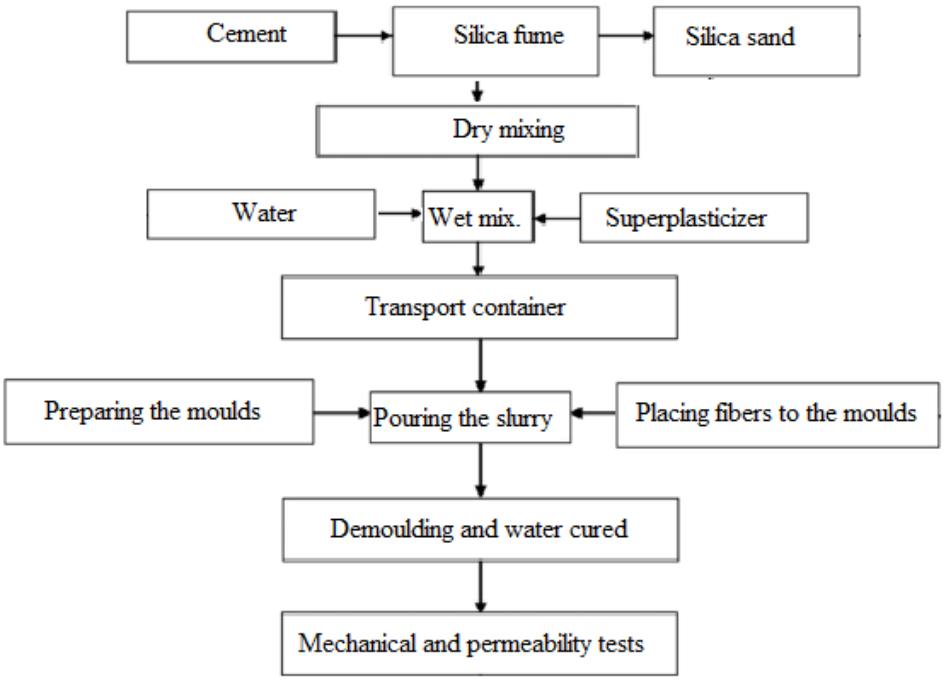

Fig. 2. Schematic flow diagram of water cured SIFCON.

Fig. 3. Preparation of test samples.

In the study, 6 pieces of 100*100*500 mm prism specimens were prepared for bending tests in each SIFCON mixture, and after bending tests compressive strength and splitting tensile strength tests were performed on the remaining specimens at 100*100 mm² cross section. In addition, capillary water absorption tests were also carried out on some beam samples.

2.3. Fracture test procedure

3-point bending tests were performed on plain concrete samples and fiber-containing SIFCON samples. The beam samples used in the tests are 100x100x500 mm in size and the test setup is given in Figure 3. In order for the loading to be controlled, the displacement velocity is

lower in plain concrete and 0.01 mm/min is used. The displacement velocity of the samples containing steel fiber and synthetic fiber was chosen as 0.0175 mm/min up to 0.5 mm deflection and then 0.1 mm/min higher until 10 mm deflection. In order to ensure that the fracture occurs in the desired cross-section in all beam specimens, notches were created in the middle of the specimens by using a diamond saw, corresponding to 40% of the beam depth. Thus, beam samples with an effective cross-sectional area of 100x60 mm were obtained.

Deviations in the middle of the beam were determined using two Linear Variable Displacement Transducers (LVDT) and the average of both measurements was taken. The load-deflection curves of both plain and fiber-containing SIFCON concrete beam samples were determined by 3-point loading tests. Crack opening displacement (CMOD) was used as a feedback variable for stable crack formation in the samples. All samples were tested in a 200 kN capacity displacement-controlled test device. In this study, the equation given below, proposed by RILEM TC-50-FMC, was used to determine the fracture energy. The fracture energies of all samples were determined by calculating the areas under the load-displacement curve. Test setup and test images are given in Figs. 4 and 5, respectively.

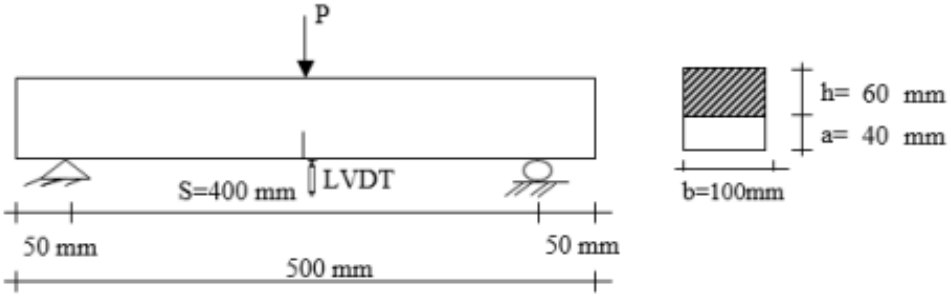

Fig. 4. Setup of the three point bending test.

Fig. 5. Displacement controlled loading test device and bending test images.

$$\frac{Wo+mg\frac{S}{L}\delta s}{B(D-a)} \quad (1)$$

where, m, L, S, a and D are the mass, length, span, notch depth, width of the beam, respectively. W_0 is the area under the load-mid span deflection curve, g is the gravitational acceleration and δ_S specified deflection of the beam (i.e. 10 mm).

The characteristic length (l_{ch}) was used for the ductility of the samples. This value was calculated using the formula proposed by Hiilerborg et al. (1976). However, in this study, splitting tensile strength values were used instead of direct tensile strength. In the equation, the modulus of elasticity was denoted by E, the fracture energy by GF, and the splitting tensile strength ft.

$$l_{ch} = \frac{E.GF}{(ft)2} \quad (2)$$

3. Tests Results and Discussion

3.1. Compressive strength

Compressive strength tests were carried out on cube samples with a side of 100 mm obtained from the samples remaining after the bending test from 100*100*500 mm beam specimens. All compressive strength tests were carried out according to EN 12390-3 standard. The results of the compressive strength tests applied to the samples as well as other mechanical behavior and permeability test results are given in Table 5.

When the compressive strength test results were examined, a small increase was observed in the compressive strength of the containing steel fiber SIFCON samples compared to the plain SIFCON samples without fiber. The most critical result is that the compressive strength of the samples using polyolefin based synthetic

fiber is significantly lower than all other samples. When polyolefin fibers are used in concrete at higher than certain ratios, they cause significant homogeneity problems. Even the very fluid mortar in the form of slurry could not flow sufficiently and homogeneously between the fibers. For this reason, the compressive strength of SIFCON samples containing polyolefin fiber is significantly lower than other all samples. While the compressive strength of the plain concrete samples is 86.2 MPa, the compressive strength of the samples containing polyolefin fiber is 66.6 MPa, and a 23% loss in compressive strength is observed with the use of synthetic fiber compared to plain samples. Similarly, in a study, the compressive strength of concrete decreases with the use of polyolefin fibers (Alberti et al. 2014). Since polyolefin fibers were used much more in SIFCON than in conventional fiber reinforced concrete, the decrease in compressive strength occurred more radically. It was observed that the compressive strength of the samples containing steel fiber increased between 1.07 and 1.14 times compared to the plain concrete samples. When polyolefin fibers are used in high amounts, the strength decreases as it becomes difficult for the slurry to flow homogeneously between the fibers.

Table 5. Mechanical and permeability properties of plain and fiber reinforced SIFCON concretes.

	Compressive strength (MPa)	Splitting tensile strength (MPa)	Flexural strength (MPa)	Fracture energy (N/m)	Chr. length (mm)	Capillary water absorption (mm)
REF	86.2	8.92	9.51	57	32	0.059
3DSF-4	98.2	17.20	36.41	12448	1945	0.083
5DSF-4	96.4	18.47	46.47	20438	2750	0.091
3DSF-8	92.1	15.29	39.46	17523	3389	0.112
PE-4	66.6	10.19	13.87	6558	2559	0.121

The modulus of elasticity is determined according to the ACI 318-14 (2014).

Coefficient of variation (C.O.V.) ranges from 1.6 % to 5.1%

3.2. Flexural and splitting tensile strength

Flexural strength tests were performed on 100*100*500 mm beam samples according to RILEM-TC-50-FCM. Then, the splitting tensile strength tests were carried out on the specimens remaining from the bending tests at an effective cross-sectional area of 100*100 mm^2 according to EN 12390-6 standard.

When the flexural strength and split tensile strength test results were examined, it was determined that there were significant increases in flexural and splitting strength in all of the fiber-containing SIFCON concrete samples compared to the plain samples. The highest bending and splitting strength values were obtained in SIFCON samples containing 5D type steel fiber, which has better adhesion to concrete and high strength. 3D steel fibers with normal strength and weaker adhesion to concrete due to their geometry have lower bending and splitting strength than samples containing 5D fibers, even when used two times by volume. As a result, it is understood that fiber strength and geometry significantly affect the bending and splitting tensile strength of SIFCON concrete.

Among the fibrous SIFCON samples, the lowest bending strength and splitting tensile strength were obtained in SIFCON samples containing polyolefin fiber. Polyolefin fibers prevent the flowable slurry from pouring completely into the molds and homogeneously dispersed. For this reason, although it increases the bending and splitting tensile strength compared to plain SIFCON samples, their bending and splitting tensile strength is much lower than SIFCON samples containing the same amount of steel fiber by volume. The use of polyolefin fibers in SIFCON concrete, even at 4% by volume, causes significant homogeneity problems. The images of some SIFCON samples containing steel fiber and synthetic fiber after bending test are given in Fig. 6. It was observed that the splitting tensile strength of the samples containing steel fiber increased between 1.71 and 2.07 times compared to the plain concrete samples. The increase in the samples containing polyolefin fiber was 1.14 times. In addition, It was determined that the flexural strength of the samples containing steel fiber increased between 3.83 and 4.89 times compared to the plain concrete samples. The increase in the samples containing polyolefin fiber was 1.46 times.

3.3. Fracture energy

The load-displacement curves of all fibrous and plain SIFCON samples produced in the study are given in Fig. 7. The highest fracture energy values were obtained in SIFCON samples containing 5D type steel fiber with high tensile strength, similar to the bending and splitting tensile strength test results. 3D steel fibers with normal strength and poorer adhesion to concrete compared to 5D fibers due to their geometry have lower fracture energy than samples containing 5D fibers, even if doubled in volume. As a result, it has been understood that fiber strength and geometry significantly affect the fracture energy of SIFCON concrete.

All fibers significantly increased the fracture energy of SIFCON concrete compared to plain concrete. It was ob-

served that the fracture energy of the samples containing 4% steel fiber increased between 218 and 358 times compared to the plain concrete samples. However, when the fiber-containing SIFCON concretes are evaluated within themselves, the lowest increases were observed in the SIFCON samples containing polyolefin fiber. This result is due to the inability of the liquid slurry to penetrate the network between the polyolefin fibers. However, samples containing polyolefin fibers have much higher fracture energy than plain concrete. By using 4% polyolefin fiber by volume, 115 times higher fracture energy values were obtained compared to plain SIFCON samples.

Fig. 6. Images of some SIFCON samples containing steel fiber and synthetic fiber after bending test.

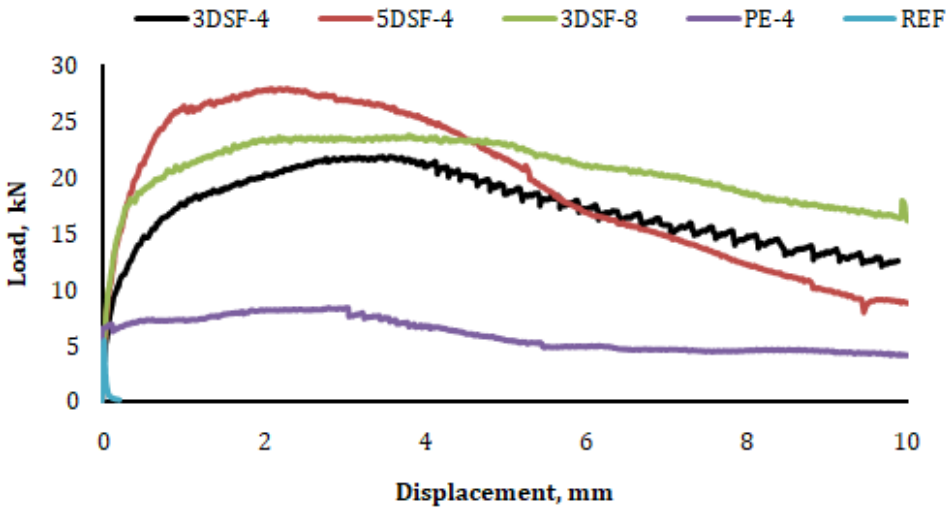

Fig. 7. Load versus displacement curves of SIFCON concrete series.

There are many studies in the literature on the use of 3D, 4D, and 5D steel fibers in concrete. The common result of all these studies is that the splitting strength, bending strength, and fracture energy values of concretes containing 5D-type high-strength steel fibers are much higher compared to concretes containing 3D and 4D-type steel fibers. This situation was associated with the hook-end geometries and high tensile strength of the 5D fibers, which provide better adhesion to concrete (Abdullah et al. 2018; Lee et al. 2019; Kizilirmak et al. 2019). The results of this study, similar to all other studies in the literature, also show that when 5D steel fibers are used in SIFCON, there is a significant improvement in all mechanical properties, especially in fracture energies, compared to the use of 3D steel fibers.

3.4. Capillary water absorption

Capillary water absorption tests were performed on the samples remaining from the bending tests. Capillary water absorption tests were carried out according to ASTM C1585 -20 (2020) standard and the amount of water absorbed by the capillary way was determined after 6 hours.

When the fibers are used in low volume ratios in concrete, there is no significant effect on the capillary water absorption of the concrete (Frazão et al. 2015). However, the fibers used above certain ratios may prevent the homogeneous distribution of the concrete. For this reason, capillary water absorption values may increase (Atiş and Karahan 2009). In this study, capillary water absorption values of all fiber reinforced SIFCON samples are higher than plain samples. It was determined that the capillary water absorption of the samples containing steel fiber increased between 1.41 and 1.90 times compared to the plain concrete samples. In the use of fiber, the diameter and amount of the gaps increase due to the problem that the concrete cannot flow sufficiently between the fiber networks. As a result, this situation increases the capillary water absorption value of the fiber-containing SIFCON samples. When the fiber-containing samples are evaluated among themselves, the capillary water absorption of the samples containing 8% by volume of 3D type steel fiber and the samples containing polyolefin is significantly higher than others. High steel fiber content or using polyolefin fiber notably increases capillary water absorption.

4. Conclusions

The results of the study can be summarized as follows:

- The compressive strength of the SIFCON samples increased slightly with the addition of steel fiber compared to the plain mixtures. However, the compressive strength of SIFCON samples containing synthetic fiber is significantly lower than plain SIFCON samples. This result is explained by the inability of the cement slurry to flow sufficiently and homogeneously into the polyolefin synthetic fiber network.
- When the splitting tensile and bending strengths of SIFCON samples are examined, the strength of all SIFCON samples increases with the use of steel fiber and synthetic fiber compared to plain samples. The highest splitting tensile strength and bending strength values were obtained in the samples using 5D type steel fibers with high strength and better adherence to concrete with their geometry.
- Fracture energies of SIFCON samples using steel fiber and synthetic fiber are significantly higher compared to plain SIFCON samples. Similar to the bending and splitting strength test results, the highest values in fracture energy values were obtained in the samples using 5D type high-strength steel fiber. Even when 5D type steel fibers are used in half the weight of normal strength 3D type fibers, higher results were obtained in all mechanical strengths and fracture energy values. Thus, it is understood that fiber strength and geometry significantly affect the mechanical behavior. The characteristic length, which is an indicator of ductility, also increases significantly with the use of fiber.
- Capillary water absorption values of SIFCON samples containing fiber are higher than plain samples. This result is explained by the fact that the fibers prevent the homogeneous distribution of the slurry. Capillary water absorption values increase significantly in mixtures containing 8% fiber, where the amount of normal strength steel fibers is very high. This shows that the use of steel fibers more than certain ratios can increase permeability. It is possible to obtain SIFCON concrete with the desired mechanical properties and low permeability by using less amount high-strength steel fibers instead of using a high amount of normal-strength steel fibers. Again, it is understood that polyolefin synthetic fibers cause problems in the flow of the slurry between the fiber network and significantly increase the capillary water absorption values.

High-strength 5D steel fibers significantly improve SIFCON mechanical properties compared to normal-strength 3D steel fibers. However, 5D steel fibers are more expensive. As a future recommendation, optimum cost-benefit analysis should be done by increasing the number of mixtures. By using the fibers in industrial products other than the laboratory environment, the properties expected from these products according to the relevant standard may also be evaluated. For example, its effects on ultimate load in infrastructure pipes, punching strength in manholes or bending strength in paving flags. In addition, the use of basalt and carbon fibers with higher tensile strength other than polyolefin in SIFCON should be considered. In this study, only macro-size steel and synthetic fibers were used. Research can be carried out in which micro and macro fibers are used together as a hybrid. Other properties of fibrous SIFCON samples such as fire performance can be examined.

Acknowledgements

The concrete specimens in the study were produced by the author while he was working at ISTON. The author also would like to thank ISTON R&D employees for their contribution.

Funding

The author received no financial support for the research, authorship, and/or publication of this manuscript.

Conflict of Interest

The author declared no potential conflicts of interest with respect to the research, authorship, and/or publication of this manuscript.

REFERENCES

Abdallah S, Fan M, Zhou X (2016). Effect of hooked-end steel fibres geometry on pull-out behaviour of ultra-high performance concrete. *International Journal of Civil, Environmental, Structural, Construction and Architectural Engineering*, 10(12), 1530-1535.

Abdallah S, Rees DW, Ghaffar SH, Fan M (2018). Understanding the effects of hooked-end steel fibre geometry on the uniaxial tensile behaviour of self-compacting concrete. *Construction and Building Materials,* 178, 484-494.

ACI 318-14 (2014), Building Code Requirements for Structural Concrete and Commentary on Building Code Requirements for Structural Concrete. American Concrete Institute, Farmington Hills, Michigan.

Alberti MG, Enfedaque A, Gálvez JC (2014). On the mechanical properties and fracture behavior of polyolefin fiber-reinforced self-compacting concrete. *Construction and Building Materials*, 55, 274-288.

Alberti MG, Enfedaque A, Gálvez, JC (2015). Improving the reinforcement of polyolefin fiber reinforced concrete for infrastructure applications. *Fibers,* 3(4), 504-522.

Ali AS, Riyadh Z (2018). Experimental and numerical study on the effects of size and type of steel fibers on the (SIFCON) concrete specimens. *International Journal of Applied Engineering Research*, 13(2), 1344-1353.

Akcay B, Ozsar DS (2019). Do polymer fibres affect the distribution of steel fibres in hybrid fibre reinforced concretes? *Construction and Building Materials*, 228, 116732.

Al-Mashhadani MMM (2021). Strength behavior of geopolymer based SIFCON with different fibers. *European Journal of Science and Technology*, (28), 1342-1347.

ASTM C1585-20 (2020). Standard Test Method for Measurement of Rate of Absorption of Water by Hydraulic-Cement Concretes. American Society for Testing and Materials, West Conshohocken, PA.

Atiş CD, Karahan O (2009). Properties of steel fiber reinforced fly ash concrete. *Construction and Building Materials,* 23(1), 392-399.

Bekaert (2021). Environmental Product Declaration Type III ITB No. 215/2021 September 07, 2022. https://www.bekaert.com

Canbaz, M, Ünüvar C (2016). Lif ve çimento türünün sifcon özeliklerine etkisi. *Pamukkale University Journal of Engineering Sciences*, 22(6), 400-404. (in Turkish)

Chen G, Zhao L, Gao D, Yuan J, Bai J, Wang W (2022). Flexural tensile behavior of single and novel multiple hooked-end steel fiber–reinforced notched concrete beams. *Journal of Materials in Civil Engineering,* 34(6), 04022077.

Ding C, Gao D, Guo A (2022). Analytical methods for stress-crack width relationship and residual flexural strengths of 3D/4D/5D steel fiber reinforced concrete. *Construction and Building Materials*, 346, 128438.

Enfedaque A, Alberti MG, Gálvez JC, Proaño, JS (2021). Assessment of the post-cracking fatigue behavior of steel and polyolefin fiber-reinforced concrete. *Materials*, 14(22), 7087.

EN 12390-3 (2019). Testing Hardened Concrete Compressive Strength of Test Specimens. European Committee for Standardization, Brussels.

EN 12390-6 (2009). Testing Hardened Concrete Tensile Splitting Strength of Test Specimens. European Committee for Standardization, Brussels.

Farnam Y, Moosavi M, Shekarchi M, Babanajad SK, Bagherzadeh A (2010). Behaviour of slurry infiltrated fibre concrete (SIFCON) under triaxial compression. *Cement and Concrete Research*, 40(11), 1571-1581.

Frazão C, Camões A, Barros J, Gonçalves D (2015). Durability of steel fiber reinforced self-compacting concrete. *Construction and Building Materials,* 80, 155-166

Gao D, Ding C, Pang Y, Chen G (2021). An inverse analysis method for multi-linear tensile stress-crack opening relationship of 3D/4D/5D steel fiber reinforced concrete. *Construction and Building Materials,* 309, 125074.

Guler S, Akbulut ZF (2022). Residual strength and toughness properties of 3D, 4D and 5D steel fiber-reinforced concrete exposed to high temperatures. *Construction and Building Materials*, 327, 126945.

Hiilerborg A, Modeer M, Petersson PE (1976). Analysis of crack formation and crack growth in concrete by means of fracture mechanics and finite elements. *Cement and Concrete Research*, 6, 773-782.

Ipek M, Aksu M (2019). The effect of different types of fiber on flexure strength and fracture toughness in SIFCON. *Construction and Building Materials*, 214, 207-218.

Khamees SS, Kadhum MM, Nameer AA (2020). Effects of steel fibers geometry on the mechanical properties of SIFCON concrete. *Civil Engineering Journal*, 6(1), 21-33.

Kizilirmak C, Aydın S, Yardımcı M (2019). Effect of the steel fibre hook geometry on the flexural properties of high strength steel fibre reinforced concretes under static and impact loading. *Journal of the Faculty of Engineering and Architecture of Gazi University,* 34(3), 1609-1627.

Lankard DR (1984). Slurry infiltrated fiber concrete (SIFCON): Properties and applications. *MRS Online Proceedings Library*, 42(1), 277-286.

Lee SJ, Yoo DY, Moon DY (2019). Effects of hooked-end steel fiber geometry and volume fraction on the flexural behavior of concrete pedestrian decks. *Applied Sciences,* 9(6), 1241.

Mohan A, Karthika S, Ajith J, Tholkapiyan M (2020). Investigation on ultra high strength slurry infiltrated multiscale fibre reinforced concrete. *Materials Today: Proceedings*, 22, 904-911.

Özalp F (2006). Ultra Yüksek Performanslı Betonların Mekanik Davranışı. *Ph.D. thesis*, İstanbul Technical University, İstanbul. (in Turkish)

Rattan A, Singh J (2018). Development of ultra high strength SIFCON. *International Conference on Sustainable Waste Management through Design*, Springer, Cham, 178-186.

RILEM 50-FMC (1985). Determination of fracture energy of mortar and concrete by means of three-point bend tests on notched beams. *Materials and Structures*, 18, 285-290.

Schneider B (1992). Development of SIFCON through applications. *High Performance Fiber Reinforced Cement Composites*, 177-194.

Sengul O (2018). Mechanical properties of slurry infiltrated fiber concrete produced with waste steel fibers. *Construction and Building Materials*, 186, 1082-1091.

Soylu N, Bingöl AF (2019). Research on effect of the quantity and aspect ratio of steel fibers on compressive and flexural strength of SIFCON. *Challenge Journal of Structural Mechanics*, 5(1), 29-34.

Sun G, Tong S, Chen D, Gong Z, Li Q (2018). Mechanical properties of hybrid composites reinforced by carbon and basalt fibers. *International Journal of Mechanical Sciences*, 148, 636-651.

Tagnit-Hamou A, Vanhove Y, Petrov N (2005). Microstructural analysis of the bond mechanism between polyolefin fibers and cement pastes. *Cement and Concrete Research*, 35(2), 364-370.

Topcu IB, Canbaz M (2007). Effect of different fibers on the mechanical properties of concrete containing fly ash. *Construction and Building Materials,* 21(7), 1486-1491.

Tuyan M, Yazıcı H (2012). Pull-out behavior of single steel fiber from SIFCON matrix. *Construction and Building Materials,* 35, 571-577.

Venkateshwaran A, Tan KH, Li Y (2018). Residual flexural strengths of steel fiber reinforced concrete with multiple hooked-end fibers. *Structural Concrete*, 19(2), 352-365.

Yalçınkaya Ç, Beglarigale A (2014). The effect of metakaolin and end type of steel fiber on fiber-SIFCON matrix bond characteristics. *Uşak University Journal of Material Sciences*, 3(1), 97-105.

Yazıcı H, Aydın S, Yiğiter H, Yardımcı MY, Alptuna G (2010). Improvement on SIFCON performance by fiber orientation and high-volume mineral admixtures. *Journal of Materials in Civil Engineering,* 22(11), 1093-1101.

Yildizel SA (2018). Mechanical performance of glass fiber reinforced composites made with gypsum, expanded perlite, and silica sand. *Revista Romana de Materiale,* 48(2), 229-235.